Institute of Biophysics
Department of Biophysical Chemistry and Molecular Oncology
Centre of Biophysical Chemistry, Bioelectrochemistry and Bioanalysis

Electroactivity of DNA and effects of DNA structure

Miroslav Fojta

A

pyrimidine bases

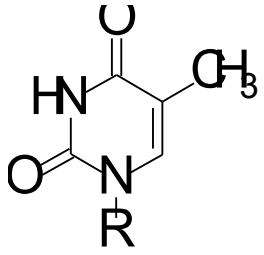

thymine (T)

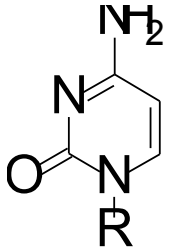

cytosine (C)

purine bases

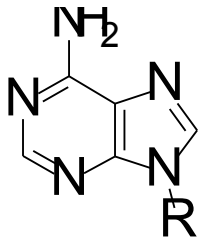

adenine (A)

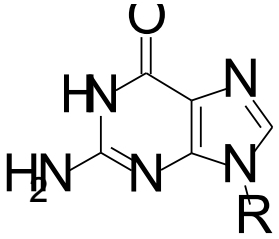

guanine (G)

B

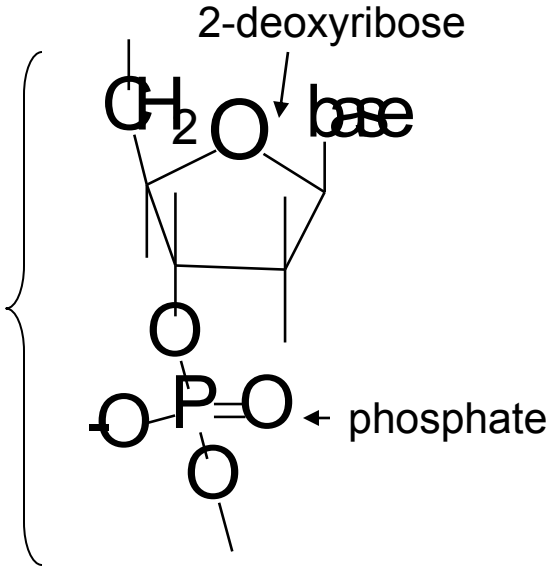

C

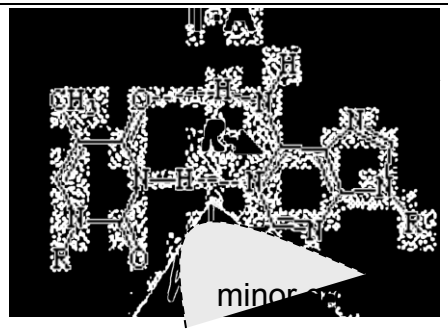

páry bazí

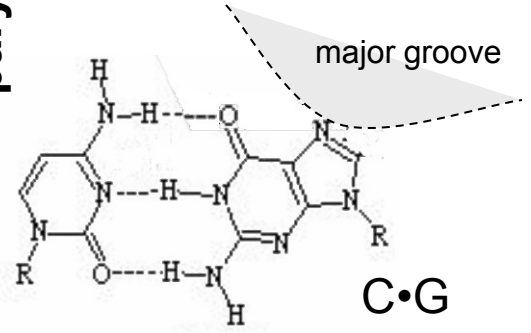

D

DNA double helix

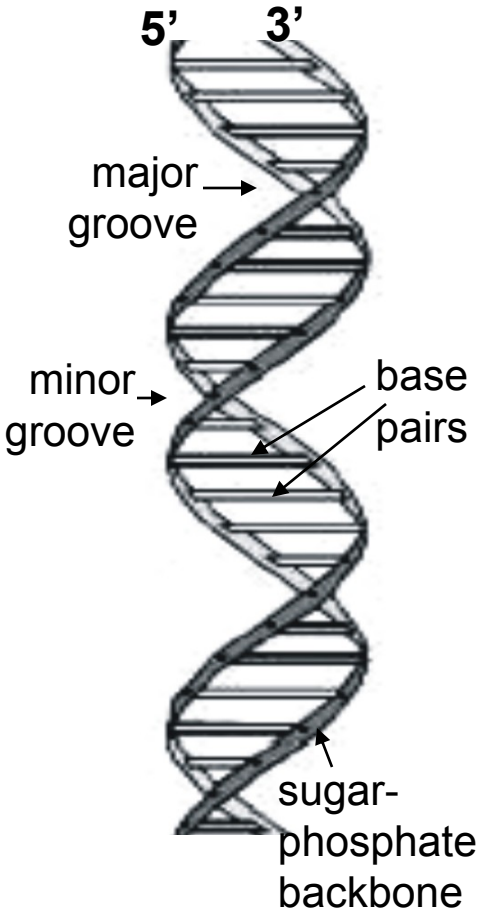

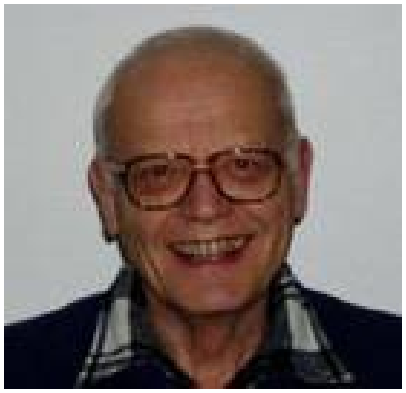

late 1950s, Emil Paleček: DNA polarography

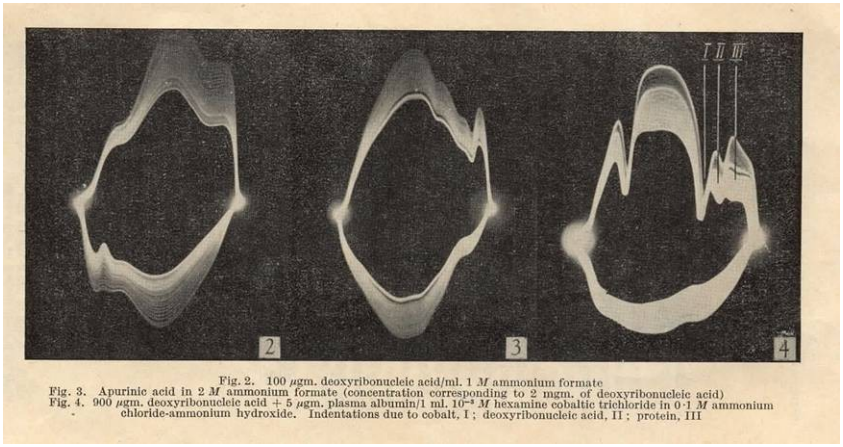

Fig. 2. 100 μgm. deoxyribonucleic acid/ml. 1 *M* ammonium formate
Fig. 3. Apurinic acid in 2 *M* ammonium formate (concentration corresponding to 2 mgm. of deoxyribonucleic acid)
Fig. 4. 900 μgm. deoxyribonucleic acid + 5 μgm. plasma albumin/1 ml. 10^{-3} *M* hexamine cobaltic trichloride in 0·1 *M* ammonium chloride-ammonium hydroxide. Indentations due to cobalt, I; deoxyribonucleic acid, II; protein, III

(Reprinted from *Nature*, *Vol.* 188, *No.* 4751, *pp.* 656-657, *November* 19, 1960)

Oscillographic Polarography of Highly Polymerized Deoxyribonucleic Acid

PROCEEDING from my finding[1,2] that nucleotides, nucleosides and the bases of nucleic acids can be analysed by alternating current oscillographic polarography[3-5], I have also tried to study polymerized deoxyribonucleic acid by this method.

The apparatus used was a Polaroskop *P* 524 (Křižík, Praha). With this apparatus it is posssible to plot dE/dt against E (Fig. 1). The analysis was carried out by means of the dropping mercury electrode in the same electrolytes as were used in my previous work[1,2]. All measurements were carried out with specimens of deoxyribonucleic acid from calf thymus.

I have established that in a medium of molar ammonium formate, deoxyribonucleic acid shows an anodic indentation at the same potential as deoxyguanylic acid (Fig. 2). Other characteristics of both indentations are also analogous (dependence on direct voltage, temperature, concentration of the electrolyte), which appears to indicate that that due to

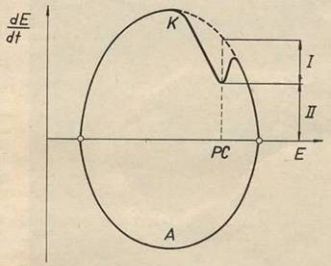

Fig. 1. Graph of dE/dt against E. The nature of the material analysed is characterized by the potential of the indentation (*PC*), which is somewhat similar to the polarographic half-wave potential. The quantity of the material is characterized by the depth of the indentation. For qualitative analysis, the height II, which can be measured much more easily, is generally measured. *K*, Cathodic part; *A*, anodic part

nucleic acids are electroactive

- at mercury electrodes, bases A,C and G undergo redox processes
- at carbon electrodes, purine bases can be oxidized
- sugar residues in nucleic acids can be oxidized at copper electrode Singhal, P.; Kuhr, W. G.: *Anal. Chem.* **1997**, *69*, 3552-3557; *Anal. Chem.* **1997**, *69*, 4828-4832.

Adenine and Cytosine are Reduced at the Mercury Electrode

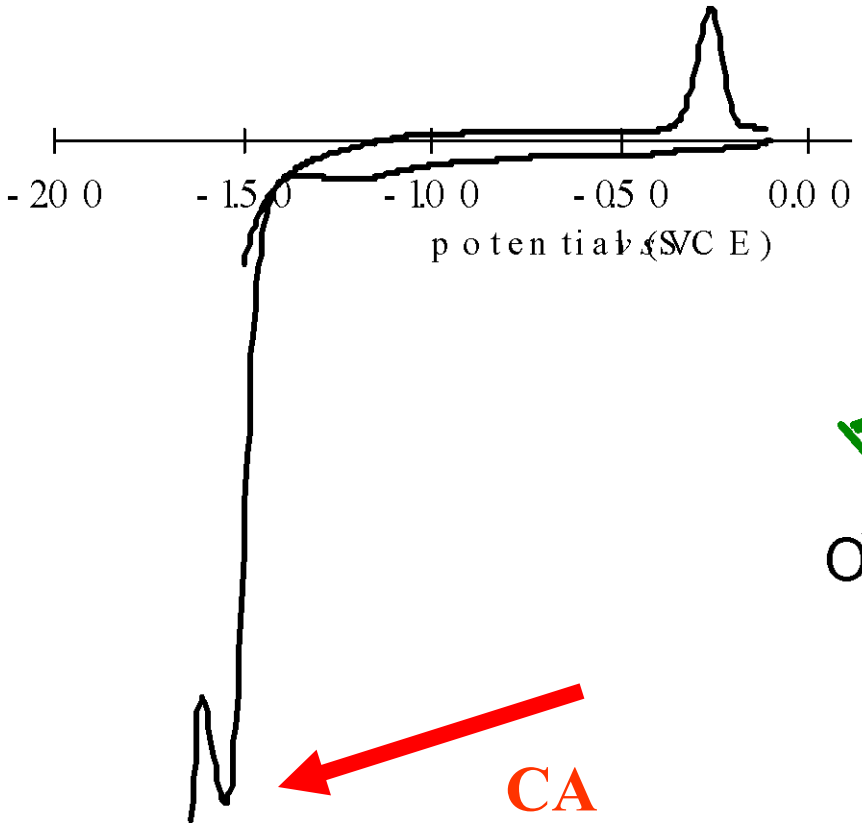

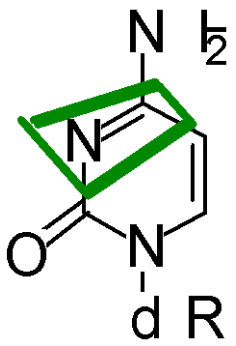

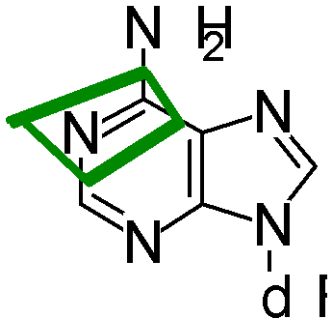

Guanine is reduced at the mercury electrode at highly negative potentials...

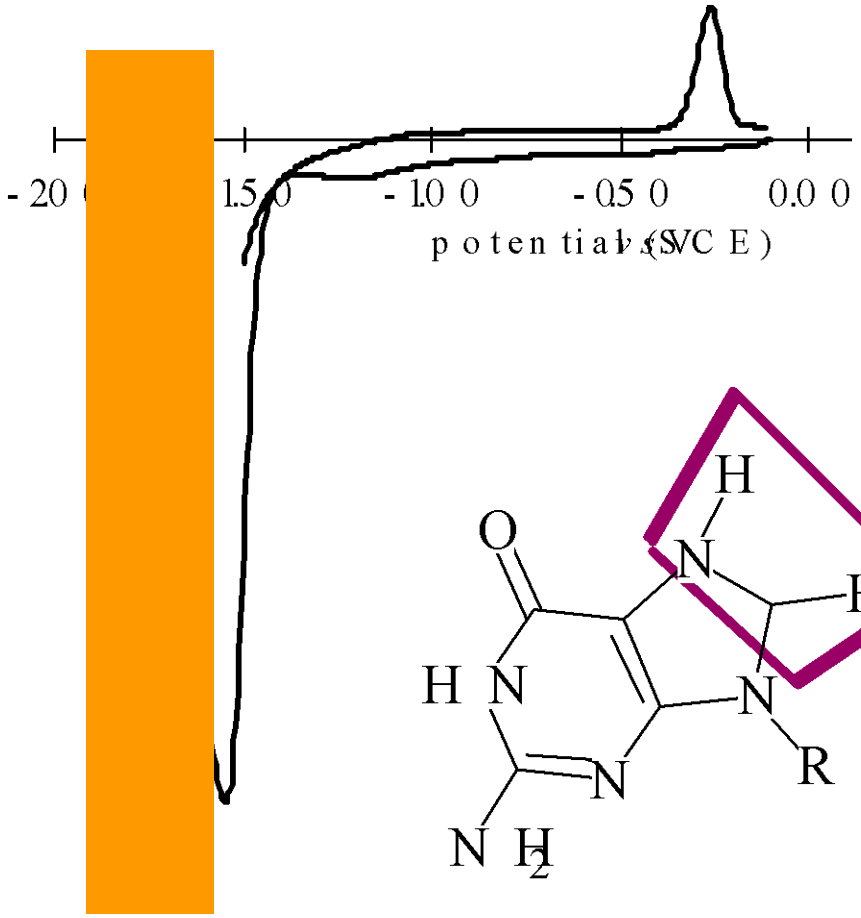

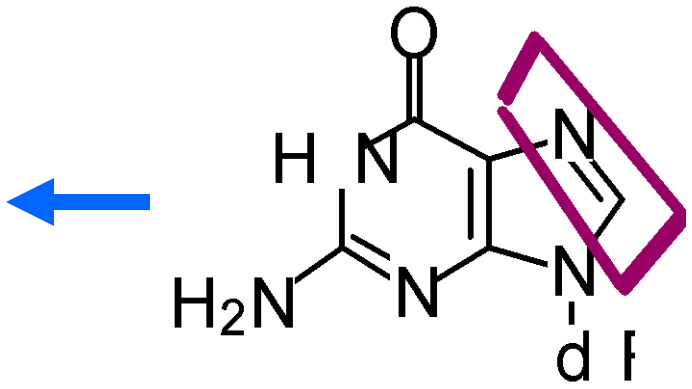

…and its reduction product yields anodic peak in cyclic voltammetry

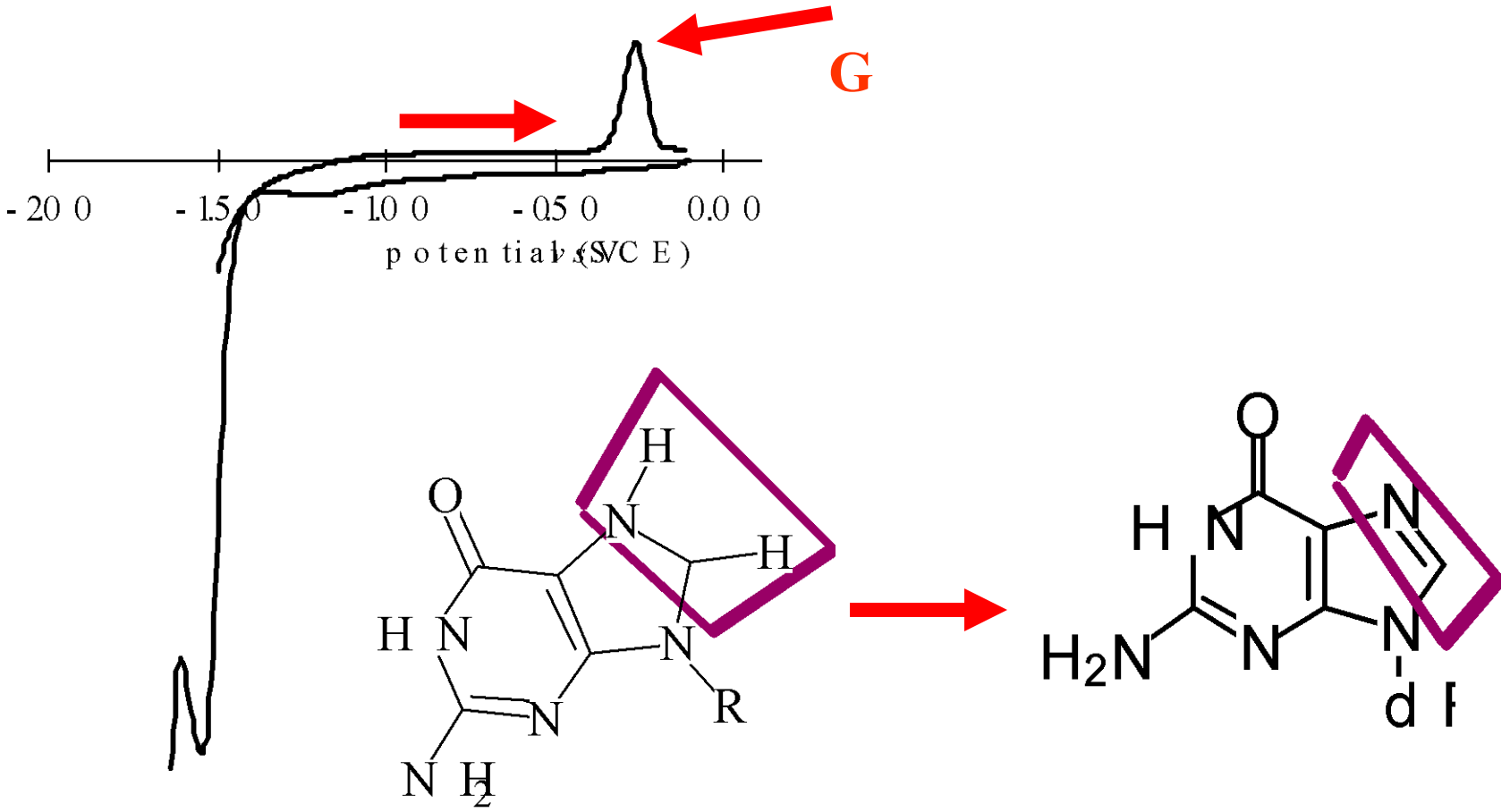

Guanine and **adenine** residues yield specific oxidation peaks at carbon electrodes

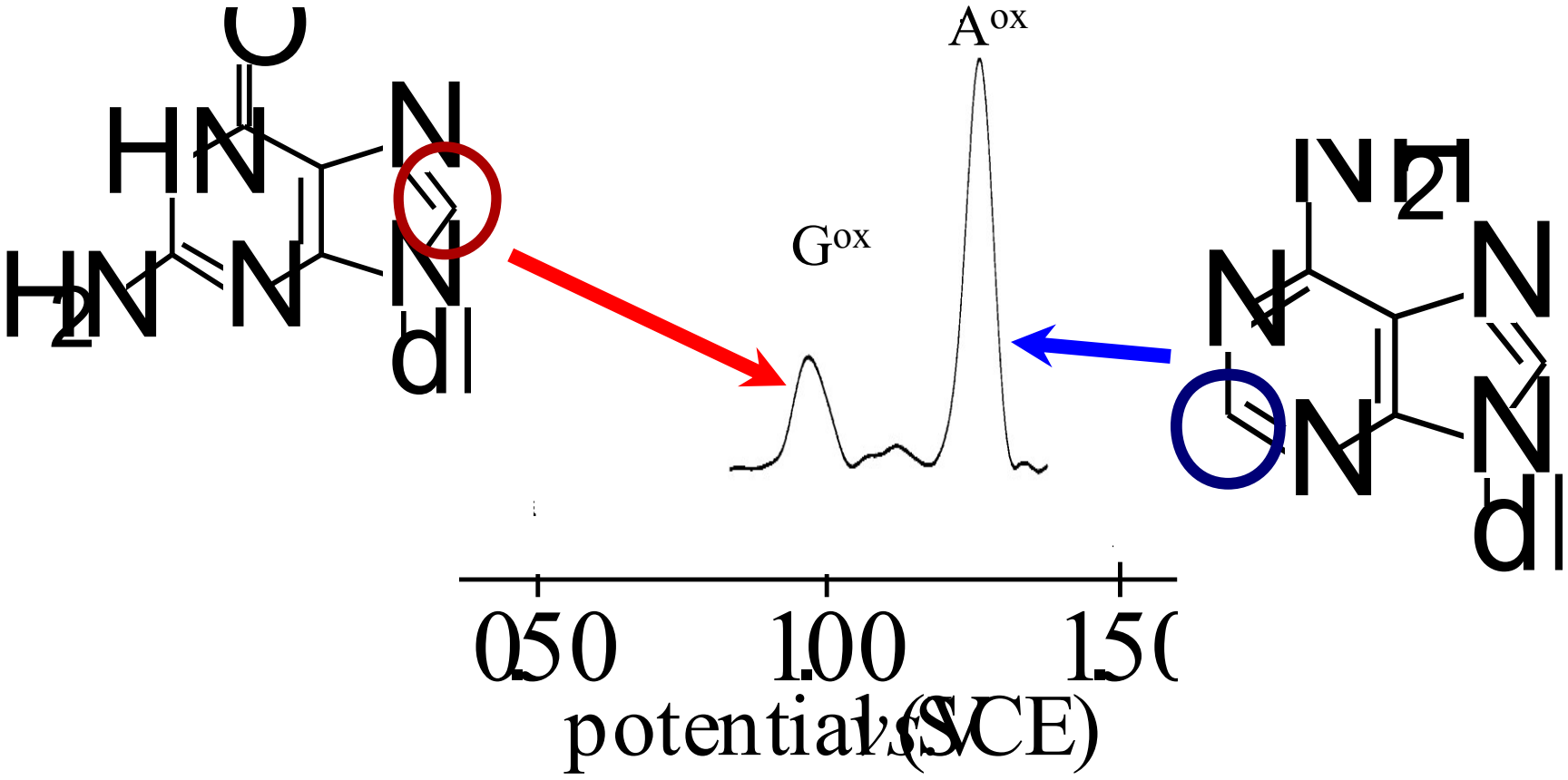

Reduction DNA signals at the
are strongly influenced by

- this is due to location of the A and C electroactiv
  within the Watson-Crick hydrogen bonding syste

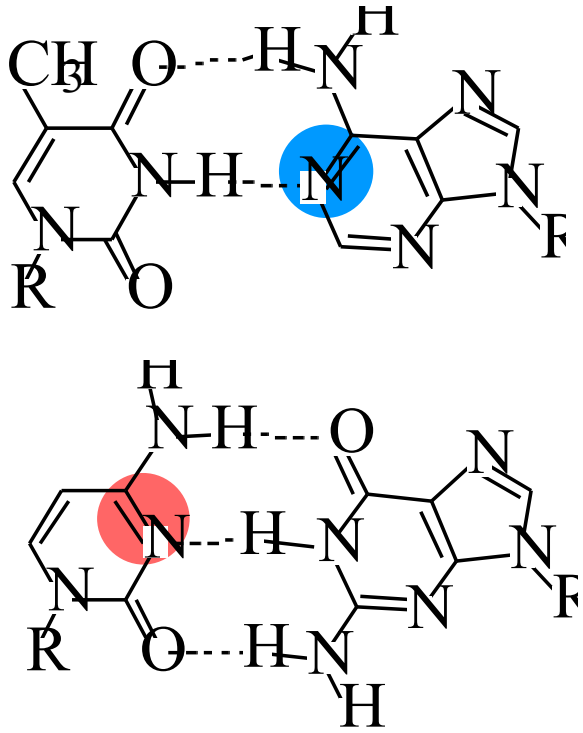

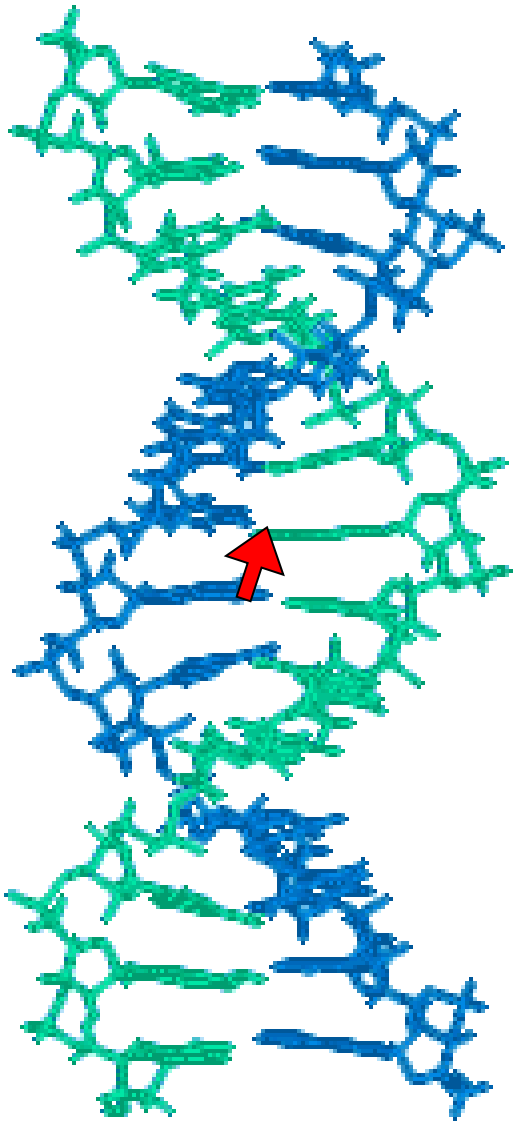

Reduction DNA signals at the mercury electrodes are strongly influenced by DNA structure

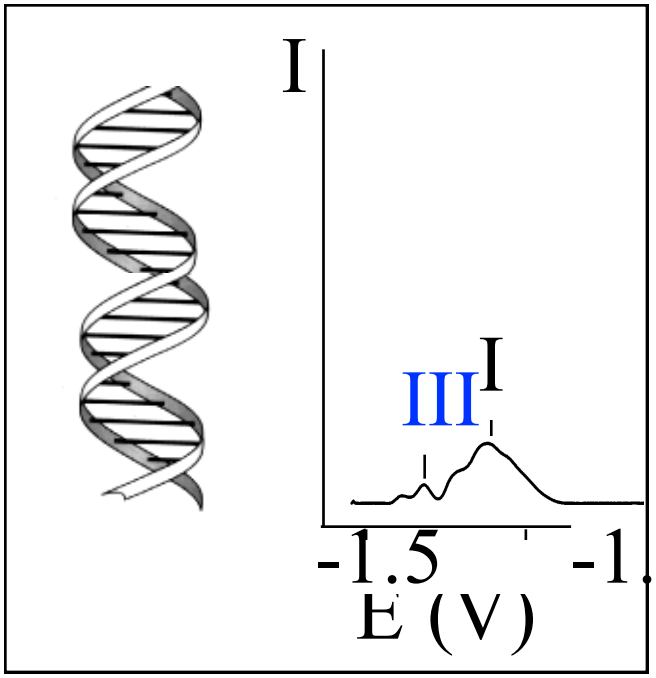

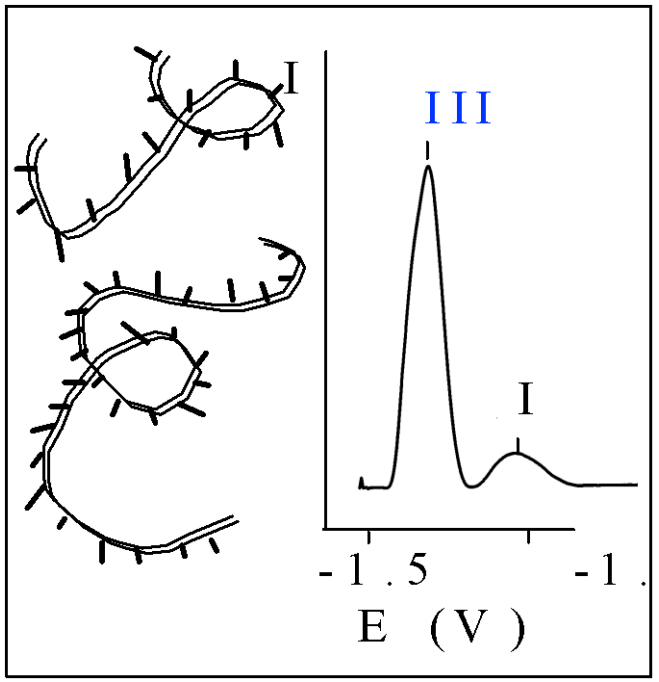

square-wave voltammetry

DNA oxidation at carbon electrodes is less influenced by DNA structure

- oxidation sites of guanine and adenine in dsDNA are located closer to the double helix surface and are accessible via the double helix grooves

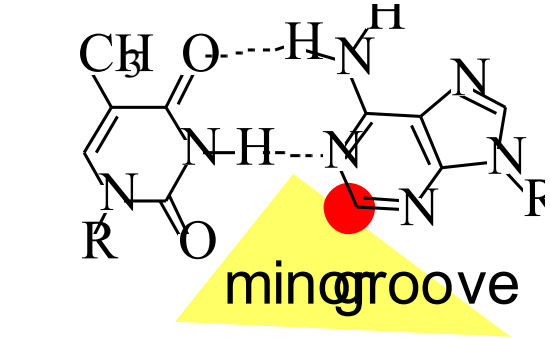

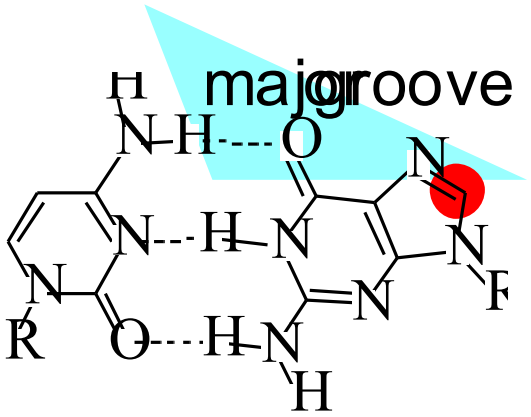

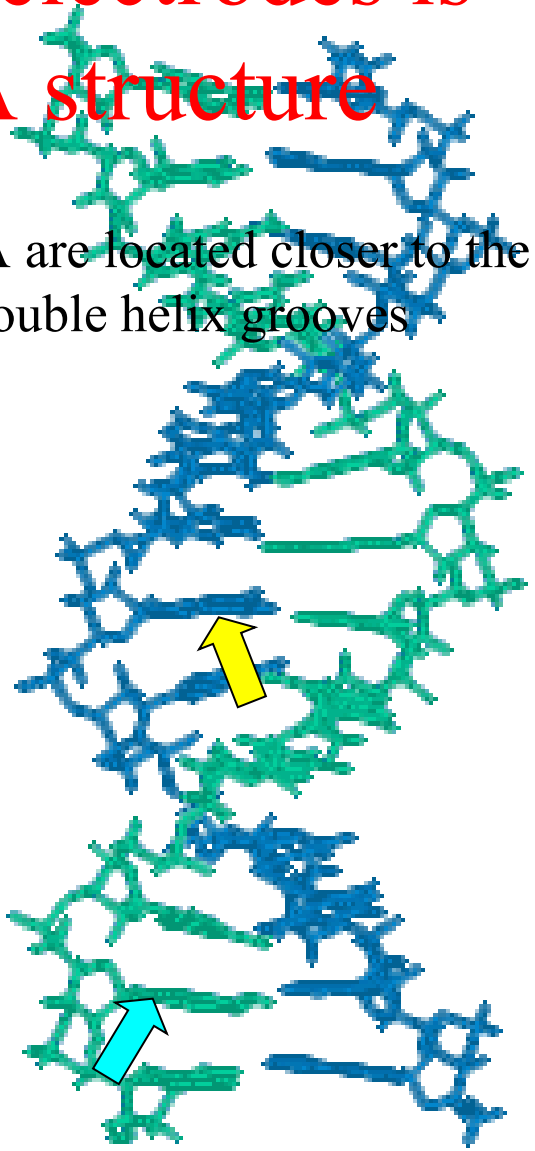

DNA oxidation at carbon electrodes is less influenced by DNA structure

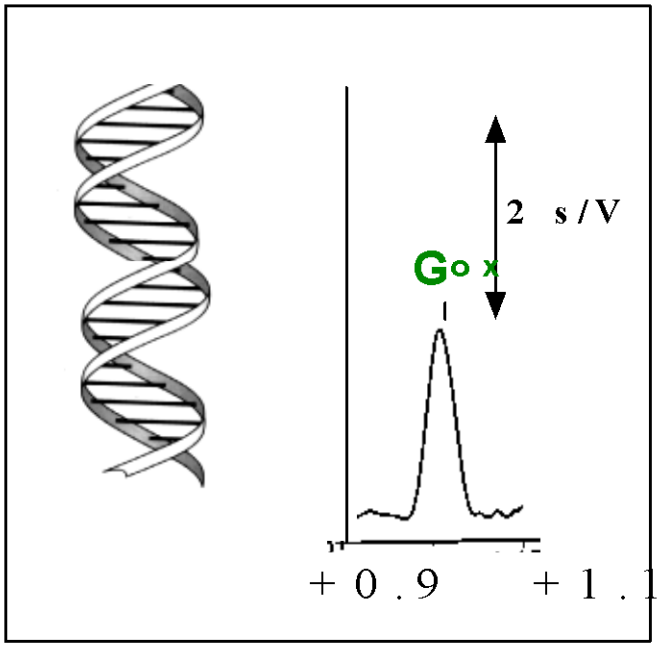

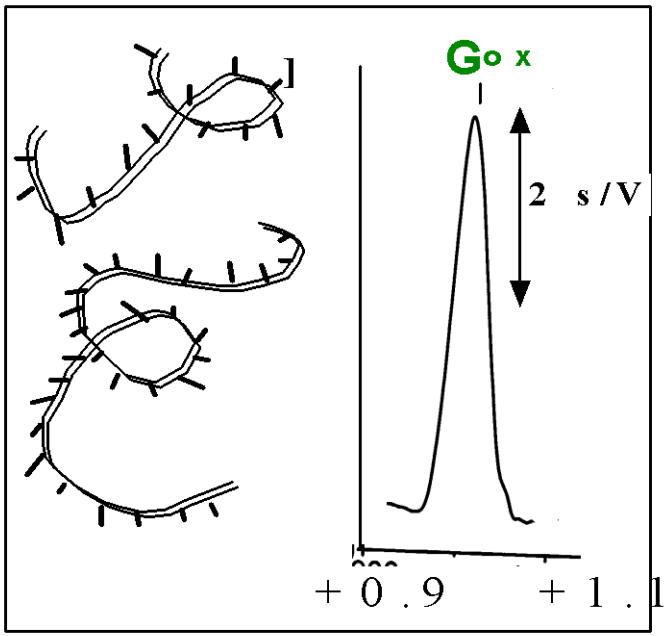

c h r o n o p o t e n t i o m e t r y

At mercury electrodes in weakly alkaline media,
adsorption-desorption (tensammetric) signals
of nucleic acids can be detected
(e.g., using AC polarography, voltammetry, AC Z)

- depending on the conditions and on DNA structure, individual components of the polynucleotide chains may be involved in adsorption/desorption processes

-at moderate ionic strenght, **double-stranded DNA** yields peak 1 due to desorption/reorientation of DNA segments adsorbed via the sugar-phosphate backbone

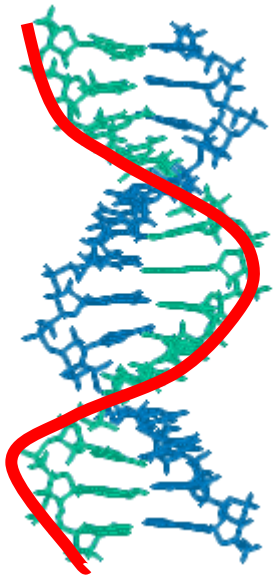

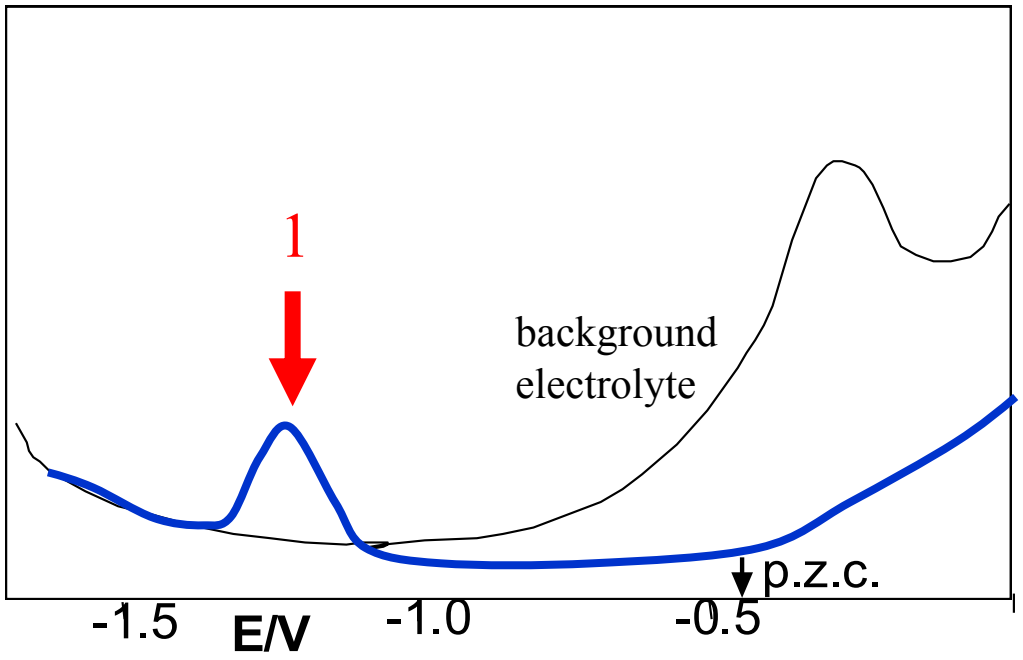

-distorted or regions of double-stranded DNA yield **peak 2**

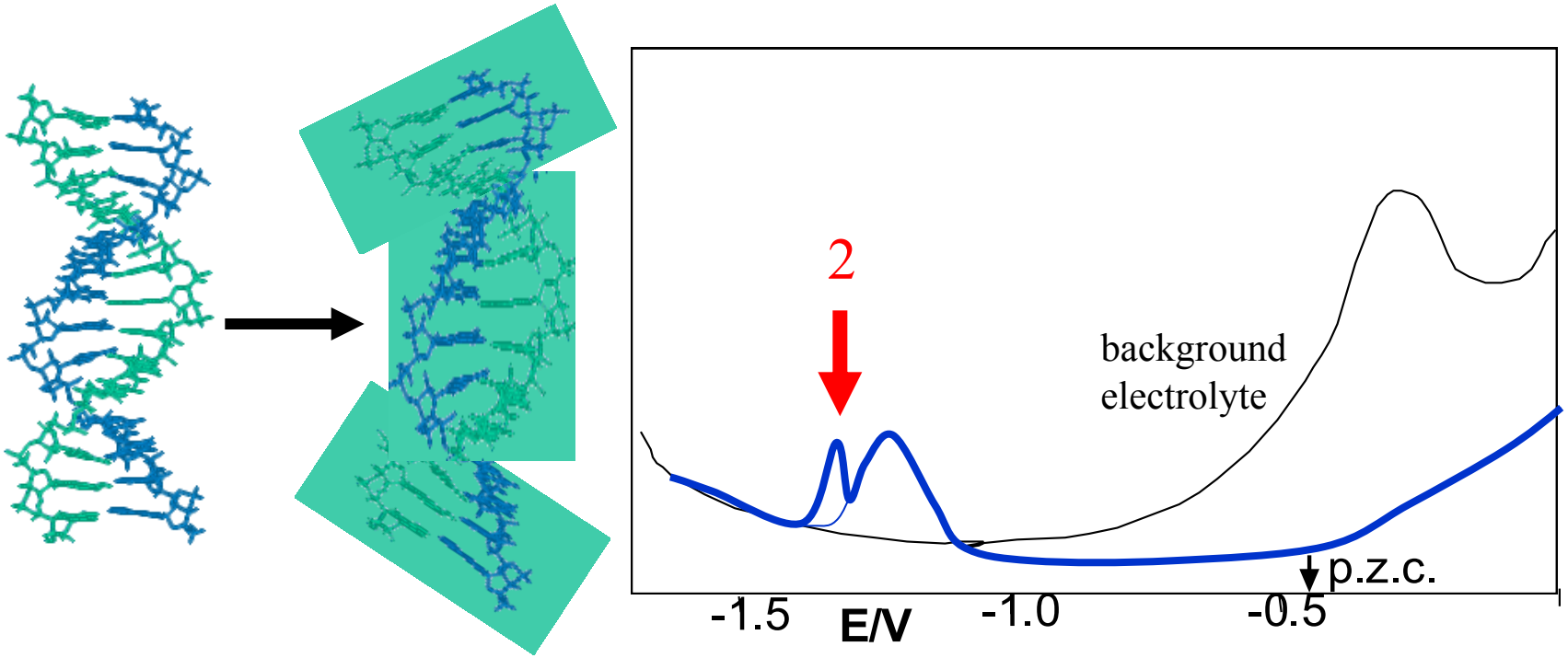

single-stranded (denatured) DNA yields peak 1 (due to the sugar-phosphate backbone) and **peak 3** due to desorption/reorientation of DNA segments adsorbed via **freely accessible bases**

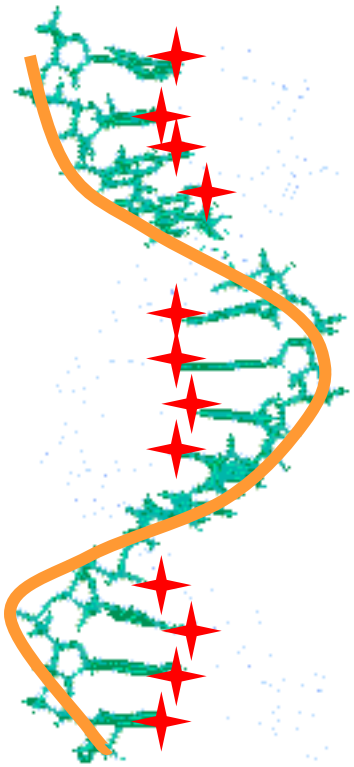

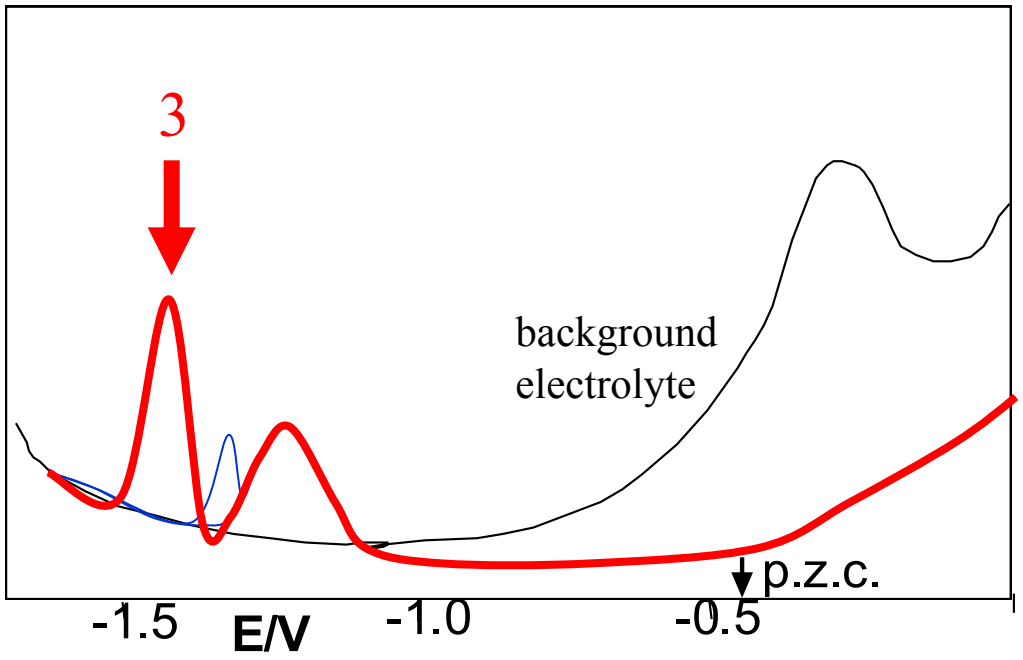

adsorption/desorption behavior of DNA at electrodes is strongly related to negative charge of its sugar-phosphate backbone
(together with a strong adsorption of nucleobases via hydrophobic forces)

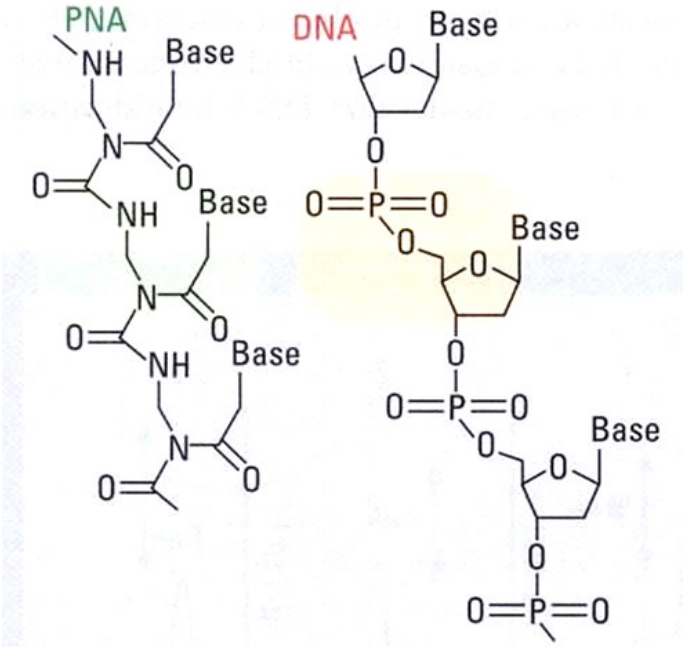

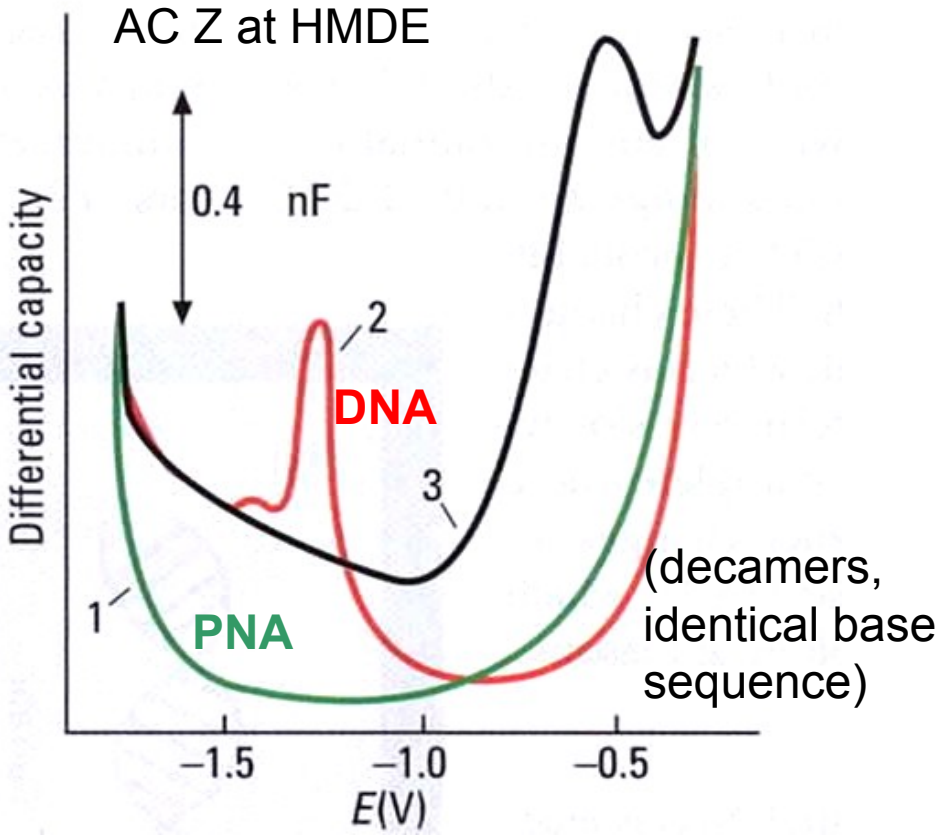

peptide nucleic acid: DNA analogue with neutral backbone

differential pulse polarography

- used in nucleic acid studies in the 60-70´s
- discrimination between ss and dsDNA

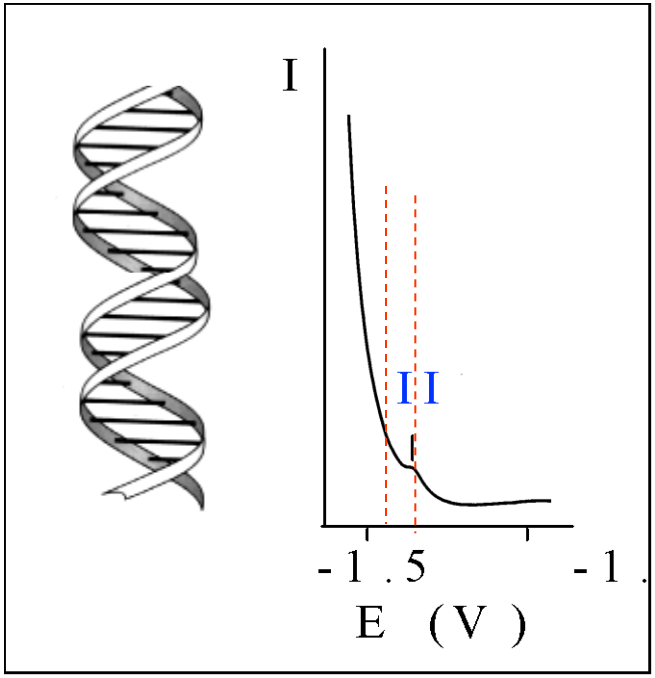

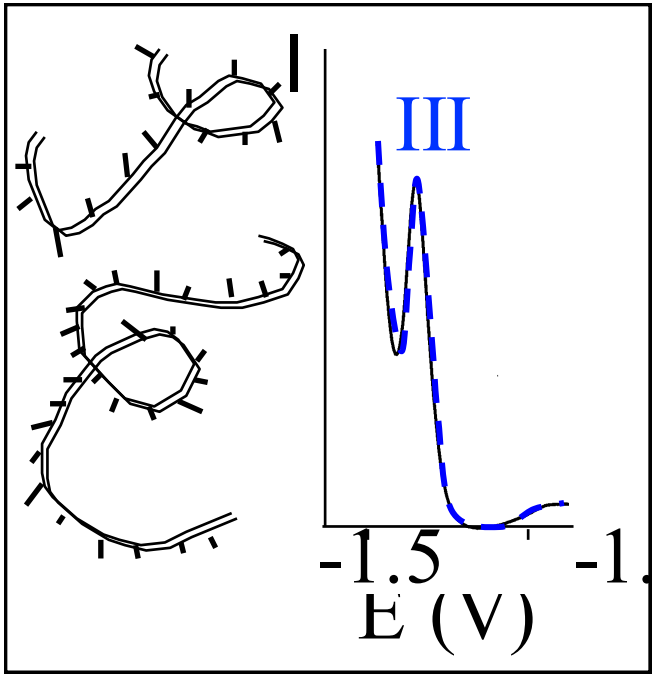

differential pulse polarography

- peak II: high sensitivity to subtle changes of dsDNA structure (&dynamics)

- DNA premelting

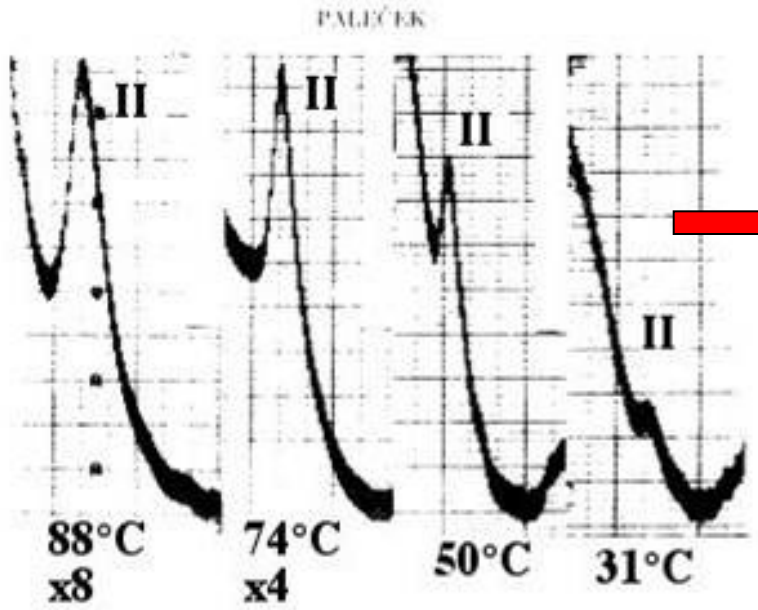

DPP peak II

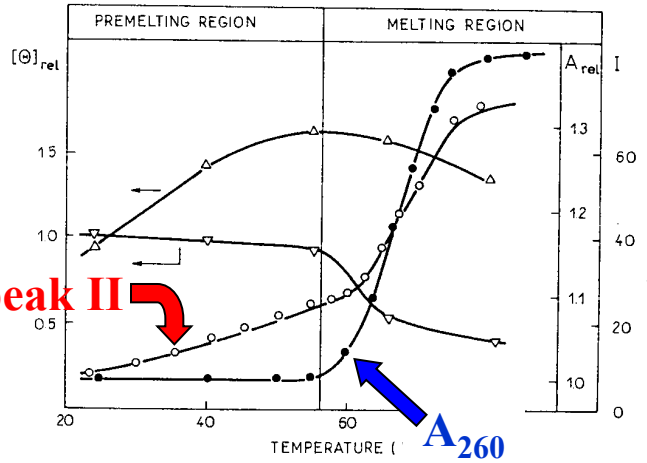

FIG. 2. Thermal transition of calf thymus DNA followed by circular dichroism (CD), derivative pulse polarography and spectrophotometry. CD: △——△, positive band (275 nm); ▽——▽, negative band (245 nm); ○——○, polarography; ●——●, absorbance at 269 nm. θ_{rel}, the ratio between the ellipticity at the given temperature and at 25°C. A_{rel}, the ratio between the absorbance (260 nm) at the given temperature and the absorbance at 25°C. I, the height of the pulse-polarographic peak in divisions. Adapted from Paleček and Frič (*21*).

[1] Nonstandard abbreviations: CD, circular dichroism; ORD, optical rotatory dispersion; ds, double-stranded; ss, single-stranded.

differential pulse polarography

- **polymorphy of DNA double helix: its structure depends on the nucleotide sequence**

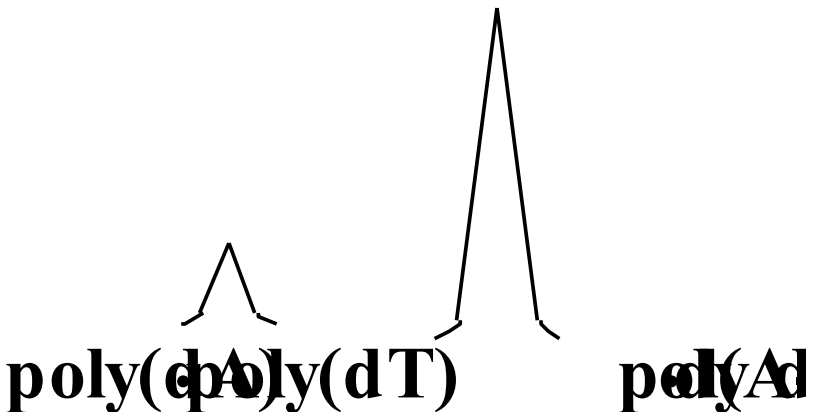

B. sublilis and B. brevis DNAs have the same G+C content and different nucleotide sequence

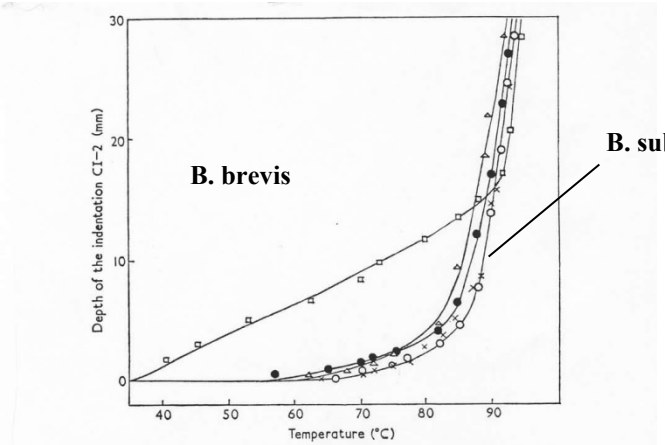

FIG. 12. Thermal transition of DNA's isolated from bacteria of the genus *Bacillus*. DNA at a concentration of 100 μg/ml. in 0·25 M-ammonium formate plus 0·025 M-sodium phosphate (pH 7·0).

—●—●—, *B. subtilis* 168; —×—×—, *B. natto*; —○—○—, *B. subtilis* var. *niger*; —△—△—, *B. subtilis* var. *aterrimus*; —□—□—, *B. brevis* (ATCC 9999).

P 524 polaroscope, dropping mercury electron polarized with repeated cycles of A.C. The measurements were carried out in the laboratory of Prof. J. Marmur, Department of Biochemistry, Brandeis University, Waltham, Mass., U.S.A.

differential pulse polarography

- **strand breaks**

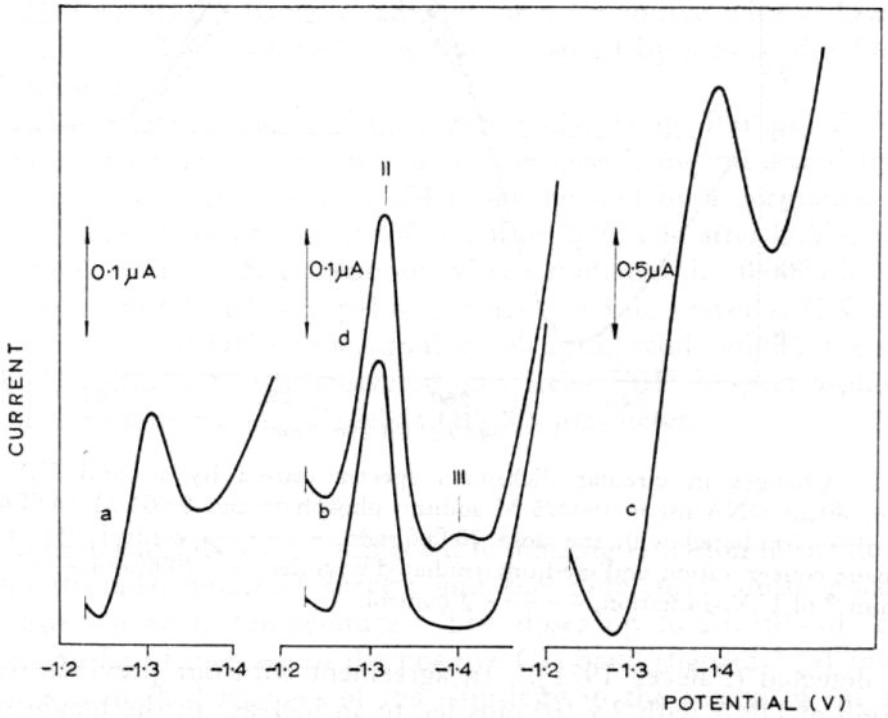

Figure 3. Differential pulse polarograms of DNA irradiated with ionizing radiation. DNA was irradiated in the concentration 460 μg/ml in the medium given in figure 1. (*a*) a control; (*b*) 10^4 rads; (*c*) 6×10^5 rads; (*d*) the sample (*b*) heated at 50°C for 6 min and quickly cooled. The differential pulse polarograms were measured in 0·3 M ammonium formate, 0·1 M sodium phosphate, pH 6·9 at DNA concentration 400 μg/ml. Sensitivity of the apparatus was 1 μA in parts (*a*), (*b*) and (*d*), and 5 μA in part (*c*).

differential pulse polarography

- **double helix distortions due to nucleobase photoadducts**

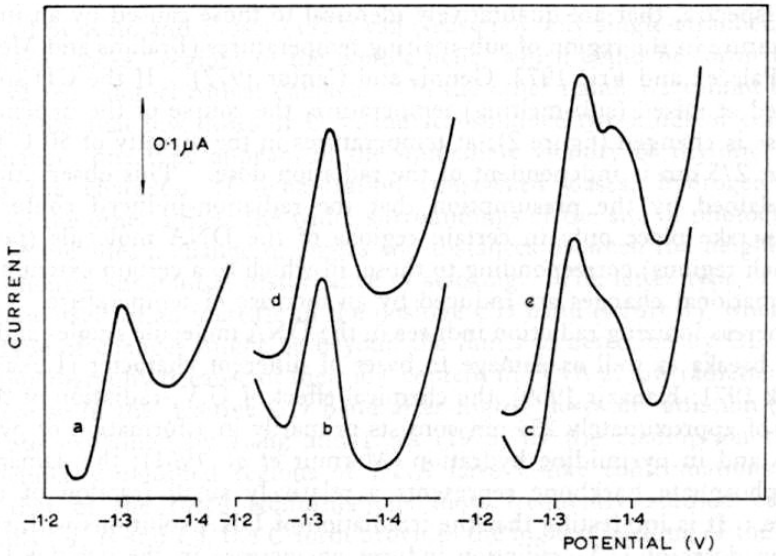

Figure 6. Differential pulse polarograms of DNA irradiated with U.V.-radiation. DNA was irradiated in the concentration 460 μg/ml in the medium given in figure 1. (*a*) a control; (*b*) $2{\cdot}1 \times 10^4$ erg mm^{-2}; (*c*) 6×10^5 erg mm^{-2}; (*d*), (*e*) the samples (*b*) and (*c*), respectively, heated at 50°C for 6 min and quickly cooled. The differential pulse polarograms were measured under the conditions given in figure 3 with the apparatus sensitivity 1 μA.

differential pulse polarography

- **chemical modification of DNA: platinum adducts**

distinction of the kind of structural change caused by modification with different Pt complexes

peak II: conformation distortion, base pairing preserved

peak III: base unpairing

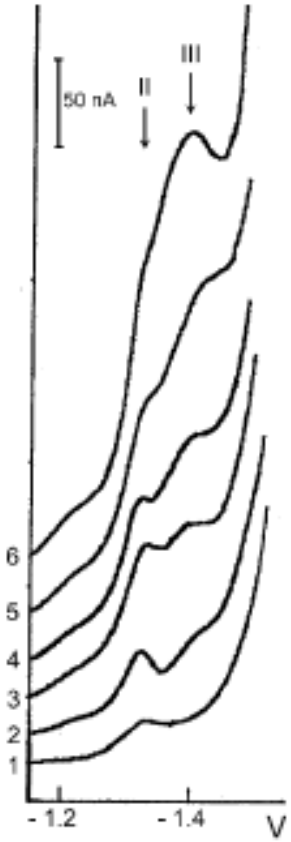

Fig. 7 Differential pulse polarographic analysis of CT-DNA modified by ORGANObisPt. DNA at a concentration of 0.4 mg/mL in 0.3 M ammonium formate with 0.01 M phosphate buffer, pH 6.8. *Curve 1*: control, unmodified DNA; *curves 2–6*: DNA modified by ORGANObisPt at $r_b = 0.001, 0.003, 0.005, 0.007, 0.01$, respectively; the *arrows* marked *II* and *III* indicate potentials *E* (against saturated calomel electrode) at which native or denatured DNA samples yielded DPP peaks II or III, respectively (see text)

(Brabec et al.)

Changes of DNA structure at electrically charged surface

DME (SMDE)

HMDE

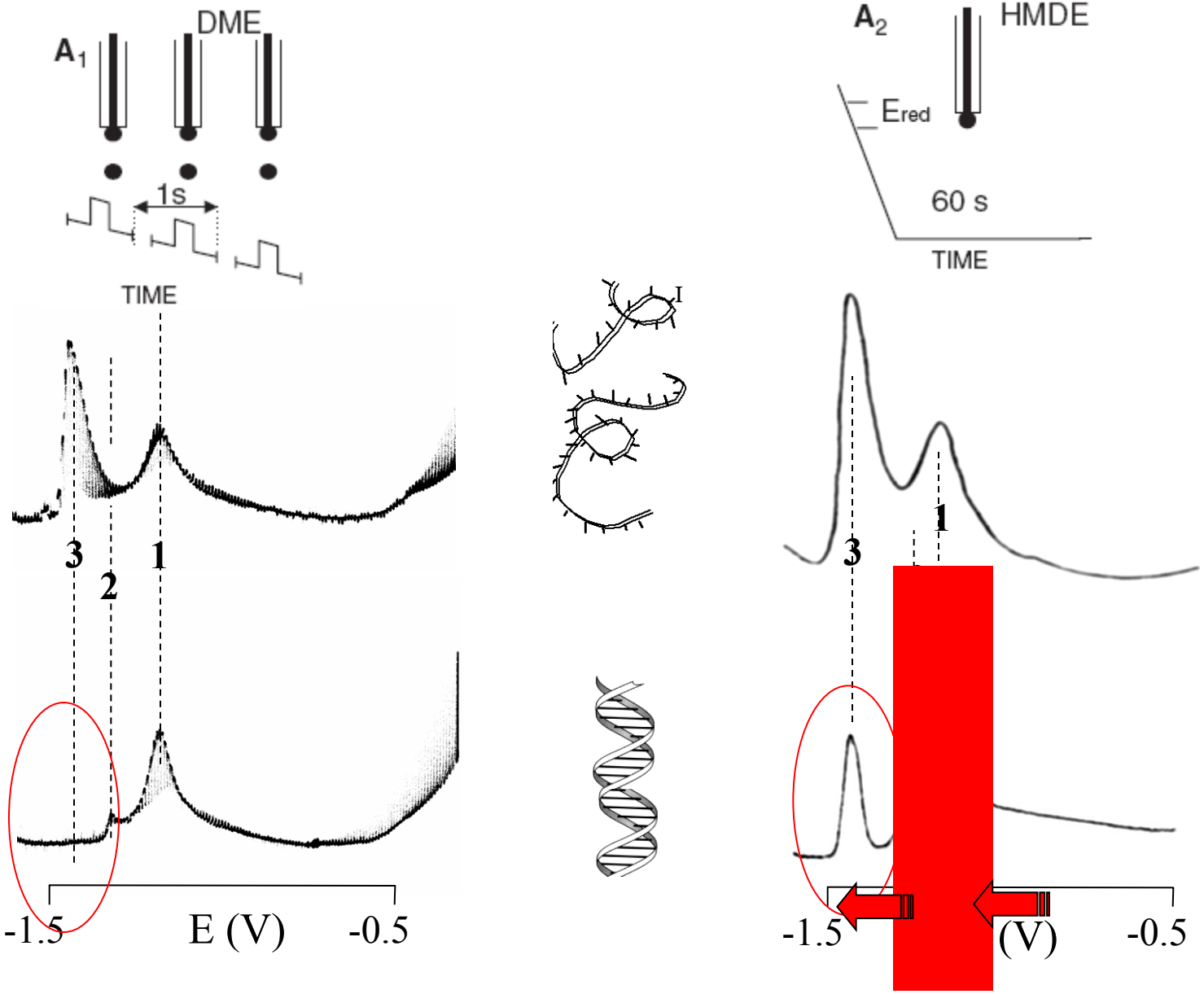

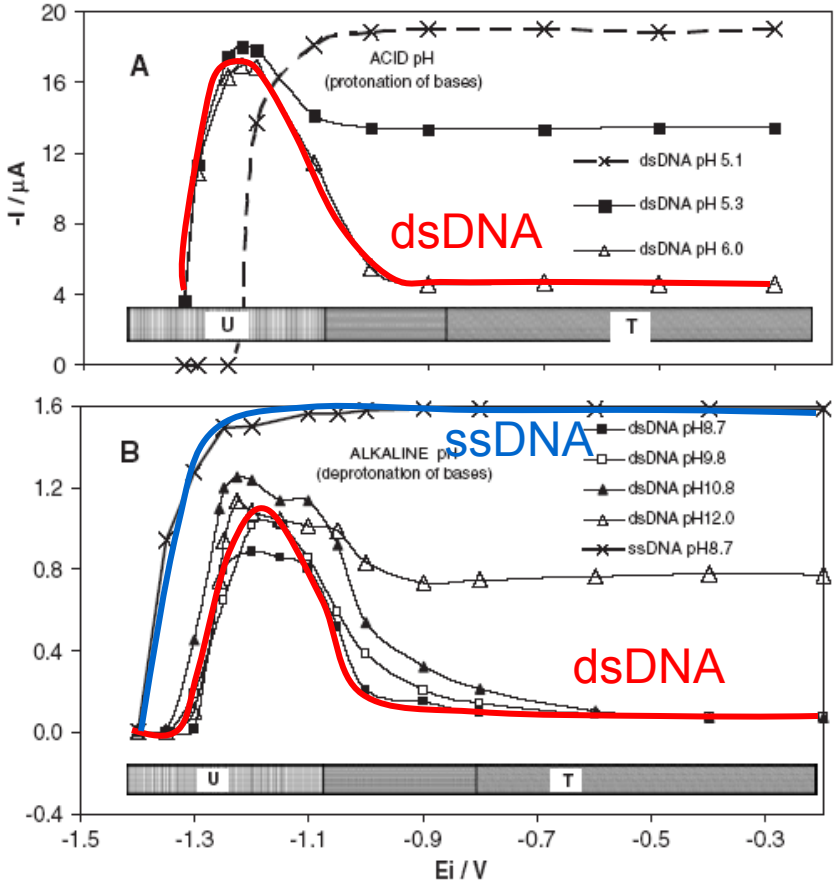

intensities of ssDNA-specific signals

prolonged exposure to
(accumulation at)
potential given on x-axis

pH close to neutral (bases not ionized):

region T: – negligible structural changes due to adsorption

region U: surface denaturation

- close to the duplex ends (or single-strand breaks), some bases can be unpaired and make contact with the mercury surface

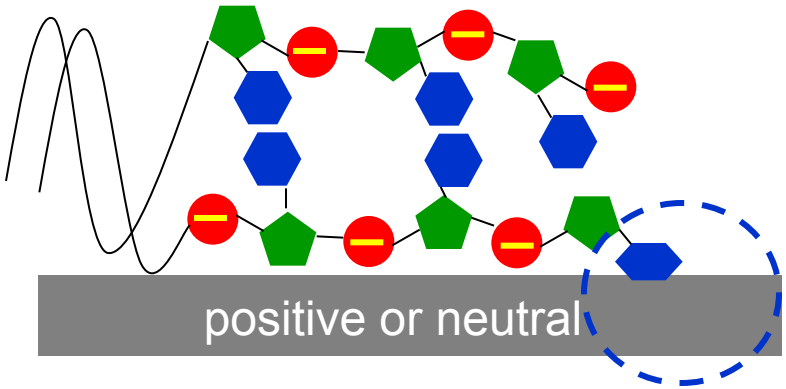

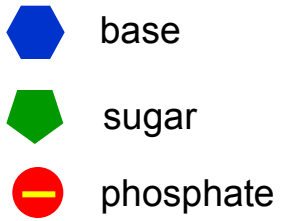

- phosphates repelled from negatively charged surface
- randomly adsorbed bases represent relatively firm anchor sites
- constraints in the double helix cause its (slow) unwinding
- more (unpaired) bases are coming into contact with the electrode

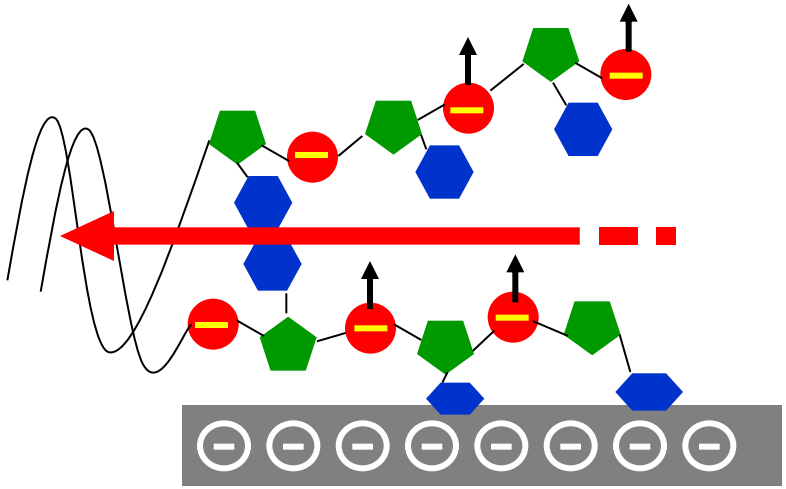

(in real situation the strand must rotate around one another; the process requires repeated adsorption/desorption events)

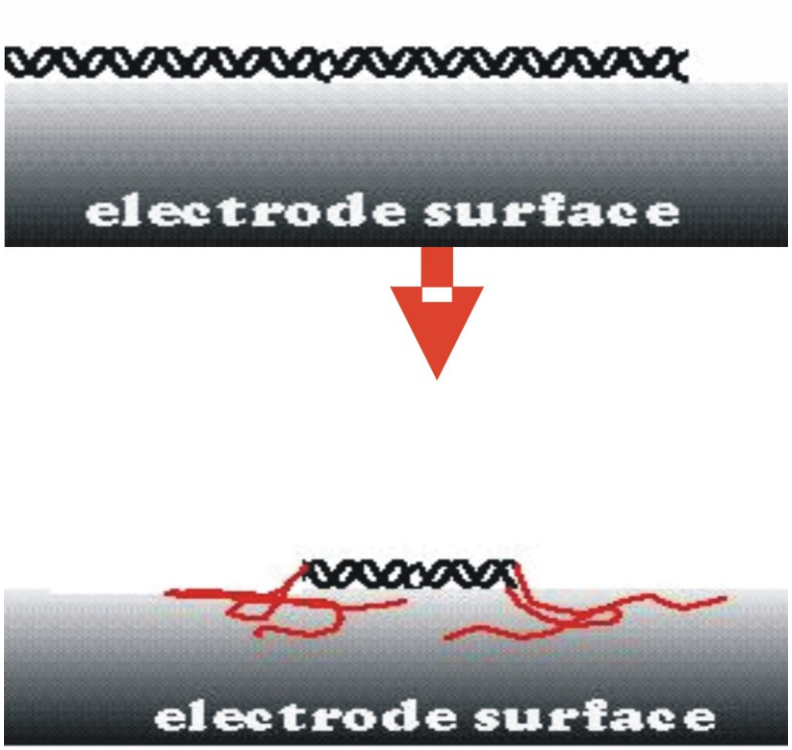
electrode surface
electrode surface

effects of initial potential and scan direction

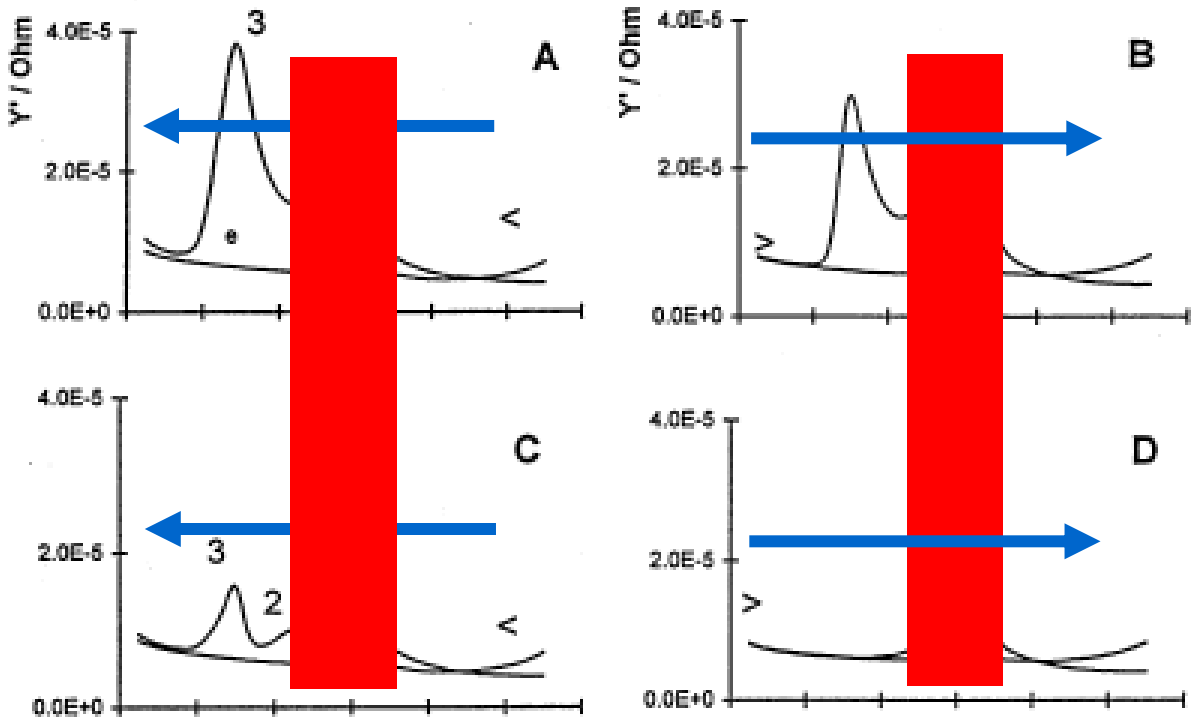

alternative models

- not double helix unwinding but conformation transition of dsDNA
- potential induced „π-state“ of dsDNA involving B-A transition at the surface (Berg)
- „ladder DNA“ structure (Nurnberg)

- these models do not accord with numerous experimental data that support the unwinding model:

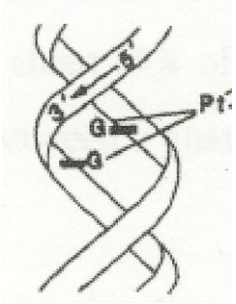

duplex with covalently cross-linked strands:
limited unwinding

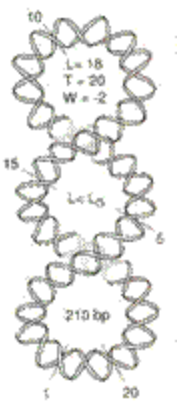

covalently closed circular DNAs:
limited unwinding

DNA with or without ends

supercoiled

open (nicked) circular

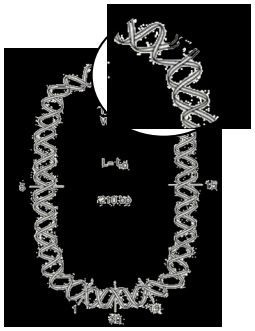

linear

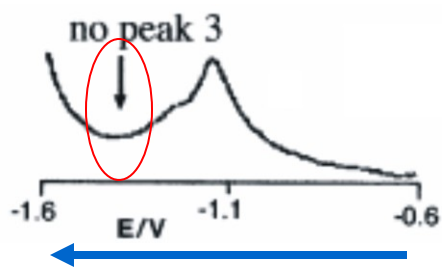

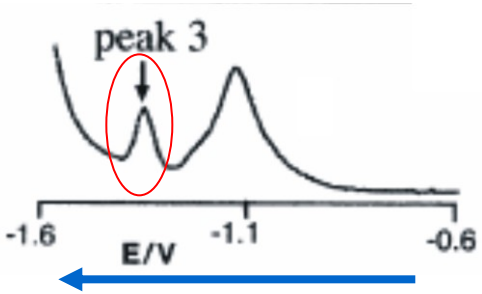

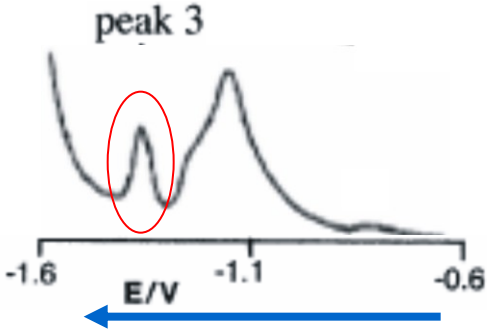

detection of DNA strand breaks using supercoiled DNA and mercury electrodes

supercoiled DNA

structural transitions induced by DNA supercoiling

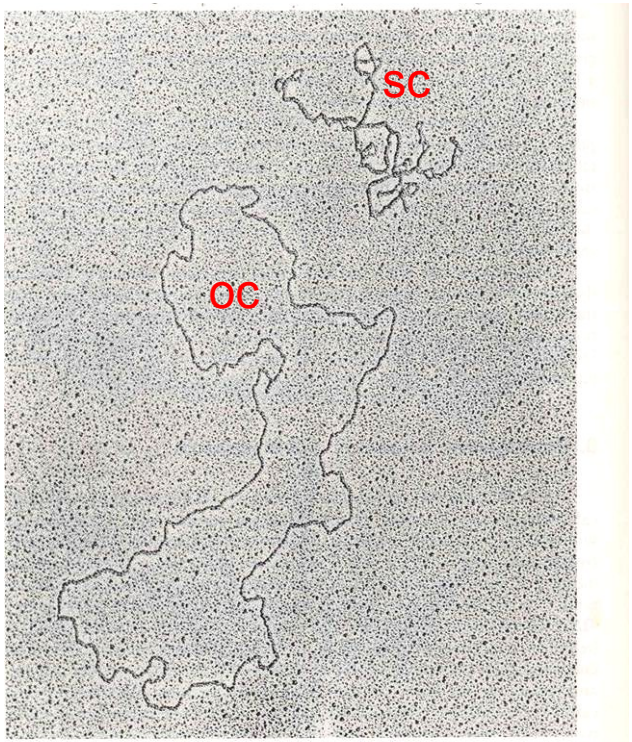

Figure 3.2 Electron micrograph of two forms of DNA. The tangled, twisted molecule is supercoiled DNA, originally called Form I DNA. When circular molecules are relaxed (or nicked) (Form II DNA), they lose the twists. A linear molecule (not shown) is called Form III. The plasmid molecules shown are 9000 bp in length. Courtesy of Jack D. Griffith.

ribbon model:

upon introducing torsional and/or bending stress, DNA behaves like an elastic ribbon

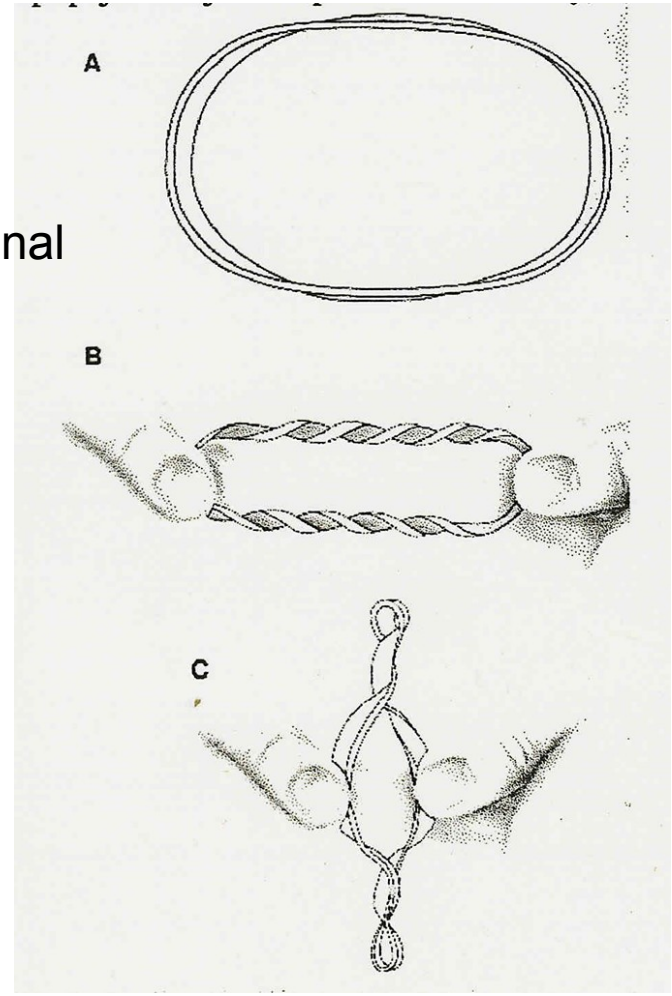

Vinograd, 1960‘s: **two forms of circular viral DNA** (sedimentation velocity or sedimentation equilibrium studies)

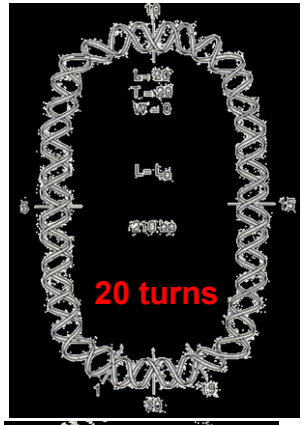

relaxed covalently closed circular DNA

(constraint due to the twist deficit causes formation of the superhelix)

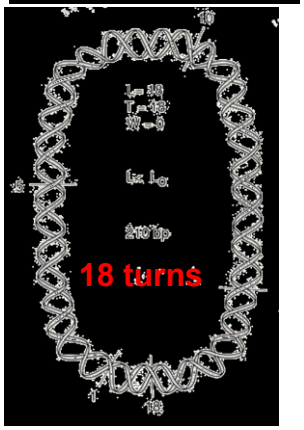

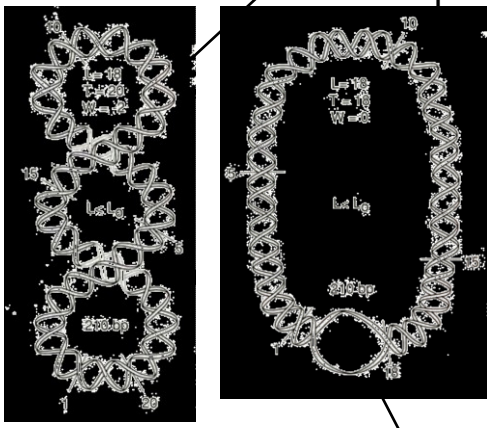

negatively supercoiled (sc) DNA

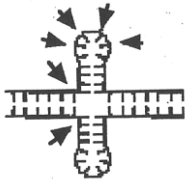

cruciform

triplex

negative superhelicty is absorbed by local opening of the double helix

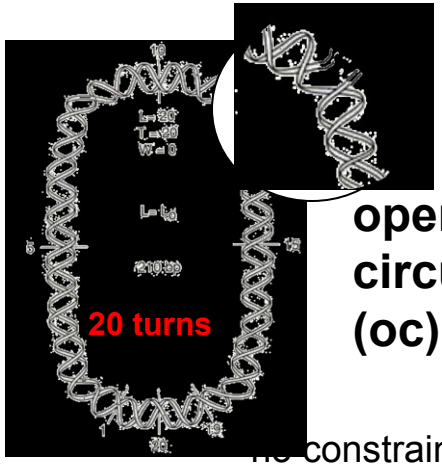

open circular (oc) DNA

no constraint – free rotation at the strand break

DNA topoisomers differ in the superhelicity level

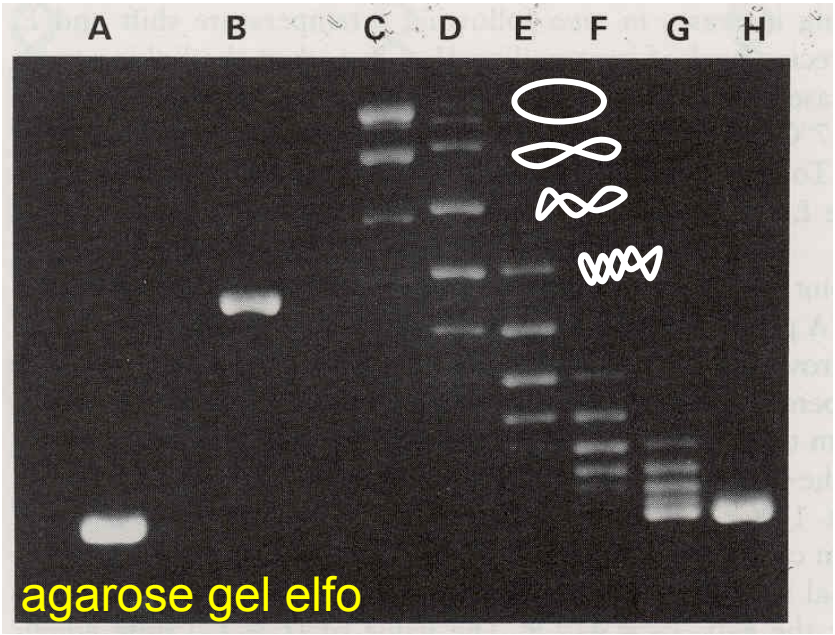

Two Superhelix Density-Dependent DNA Transitions Detected by Changes in DNA Adsorption/Desorption Behavior†

Miroslav Fojta,‡ Richard P. Bowater,§ Veronika Staňková,‡ Luděk Havran,‡ David M. J. Lilley,|| and Emil Paleček*,‡

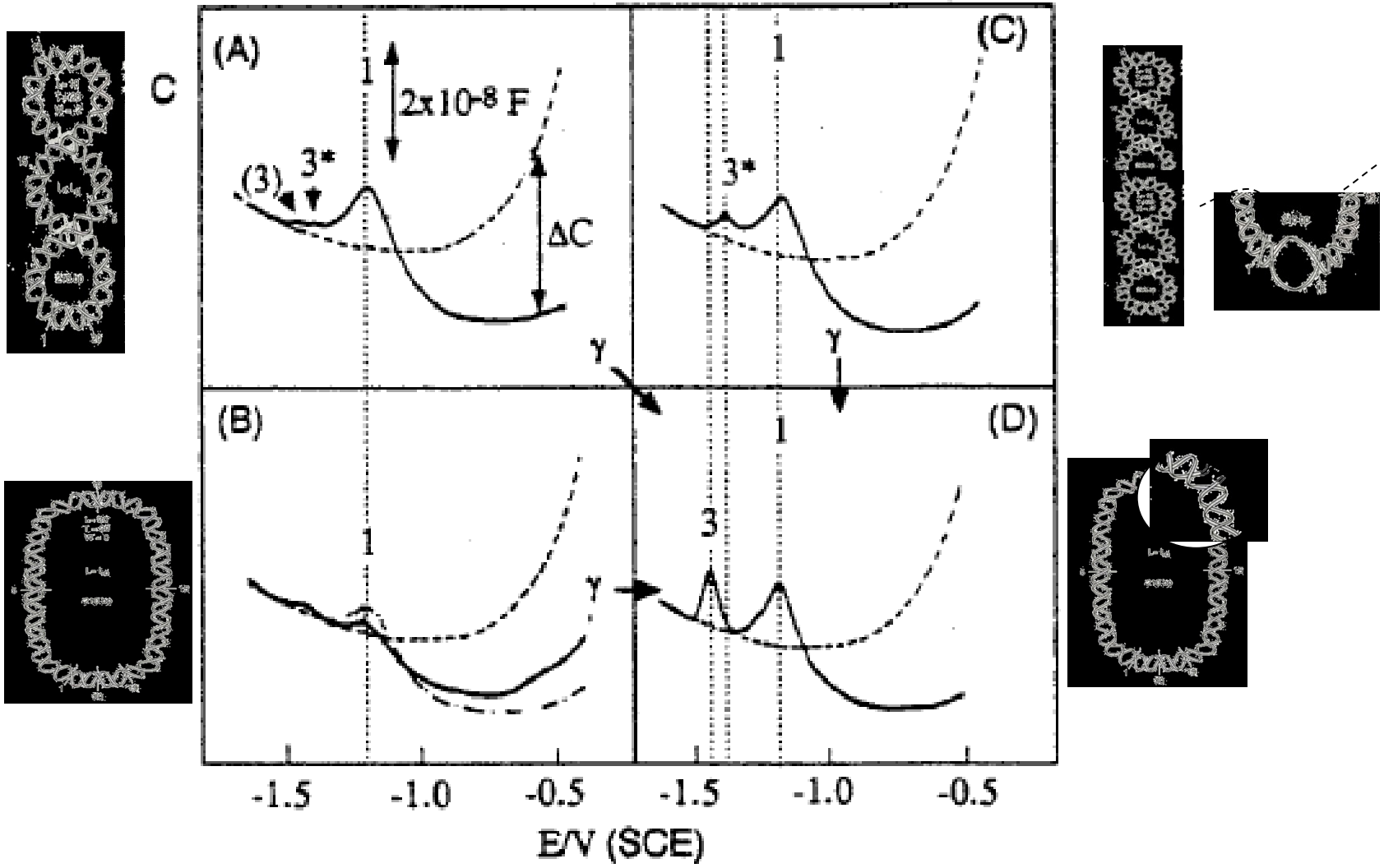

transition 1

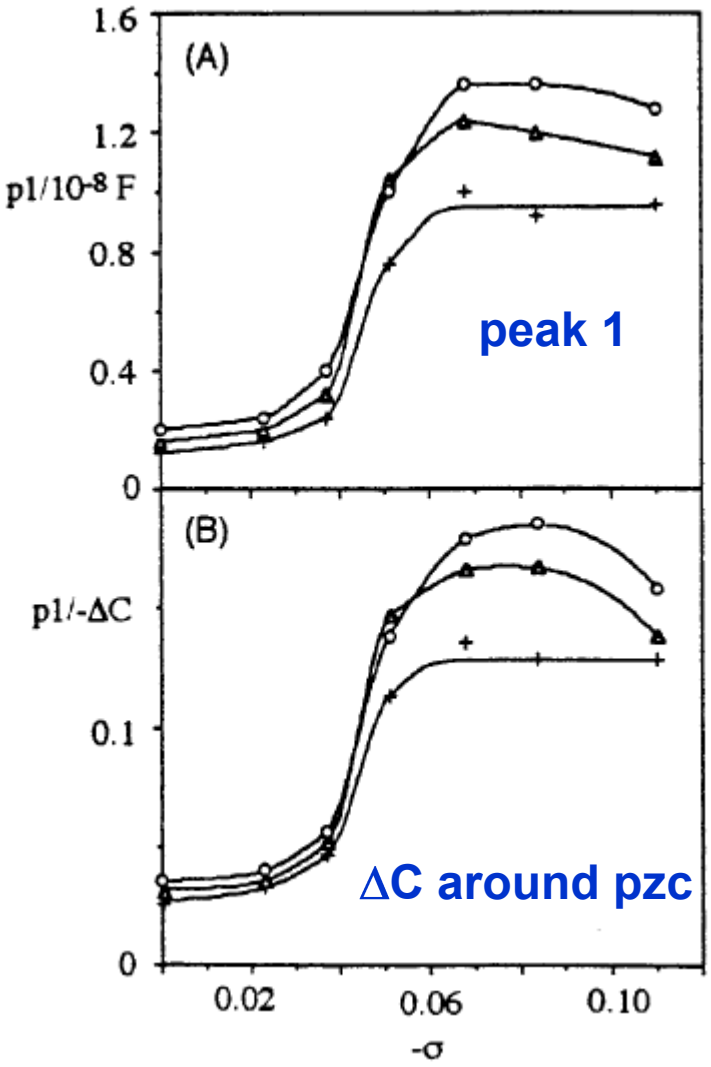

overall shape of the molecules

transition 2

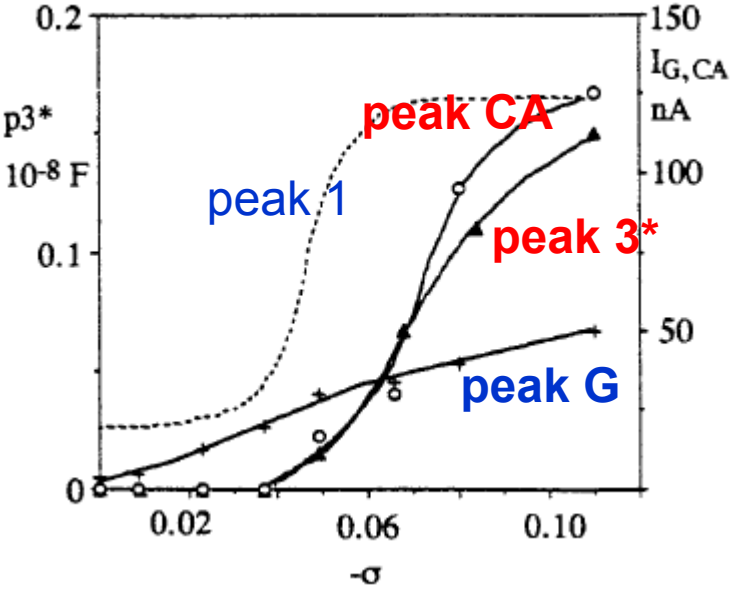

peak 3* is due to local helix opening (base unpairing)

peak CA (similar dependence on $-\sigma$ as peak 3*) is known to be sensitive to DNA denaturation

peak G (no transition 2) is less sensitive to DNA structure

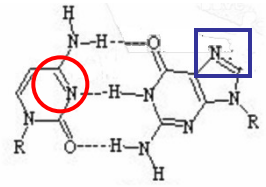

Studies with DME: peak 3* is due to helix opening in solution (in difference to peak 3 produced by oc or linear dsDNA that is observed only at the HMDE

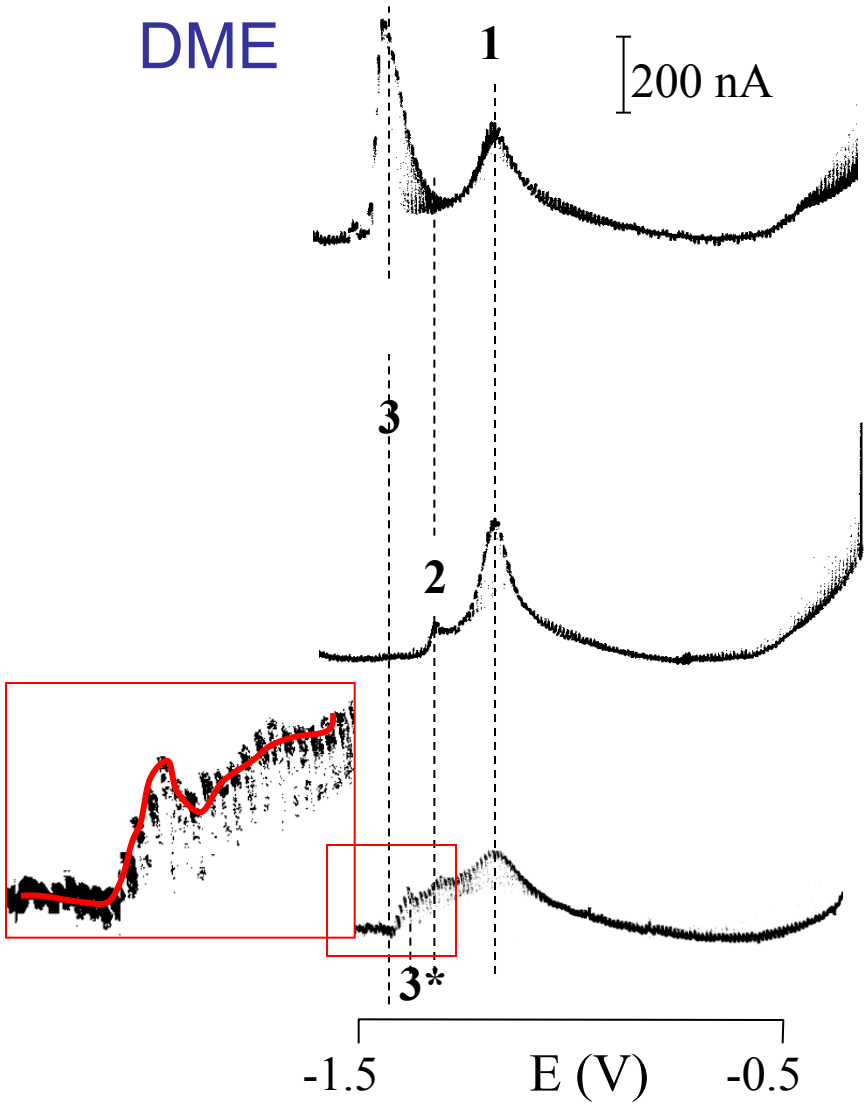

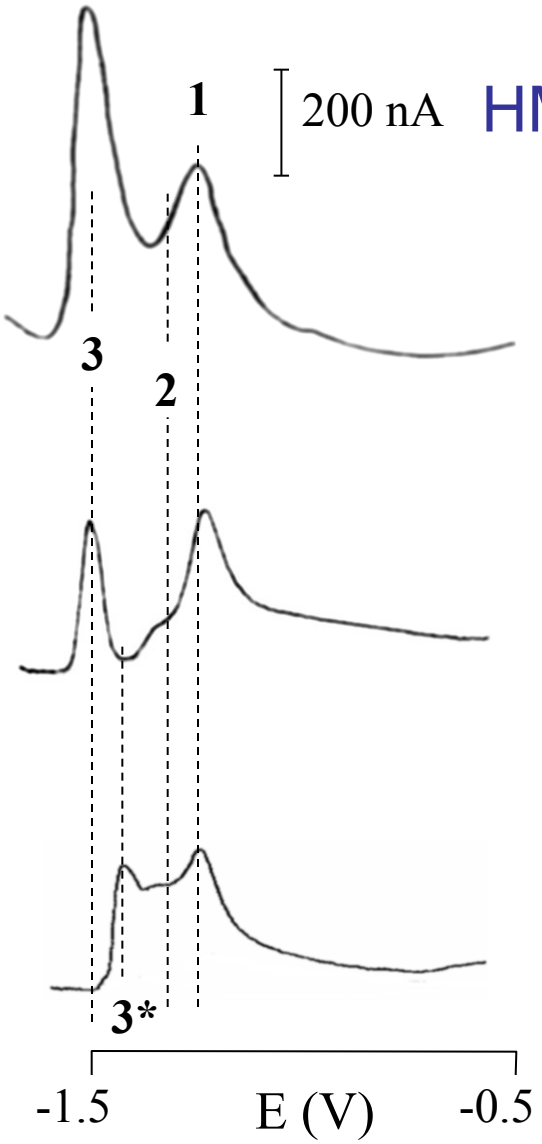

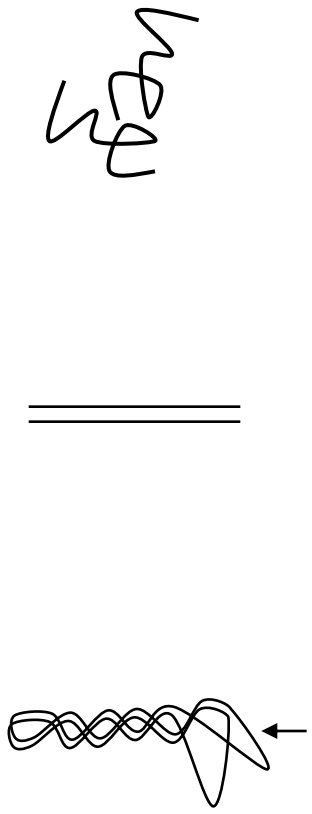

circular and linear DNAs

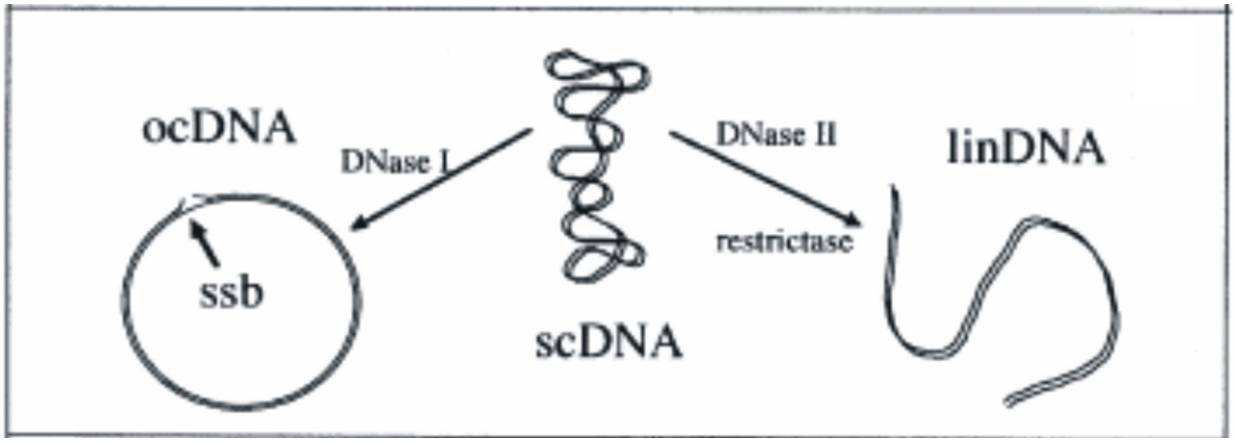
ocDNA
DNase I
ssb
scDNA
DNase II
restrictase
linDNA

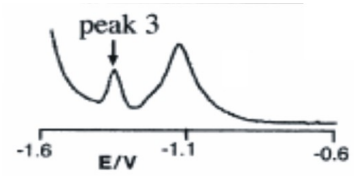
peak 3
-1.6
E/V
-1.1
-0.6

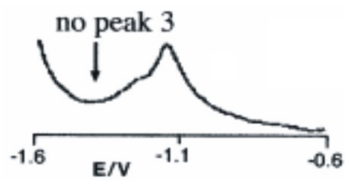
no peak 3
-1.6
E/V
-1.1
-0.6

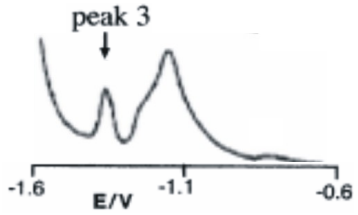
peak 3
-1.6
E/V
-1.1
-0.6

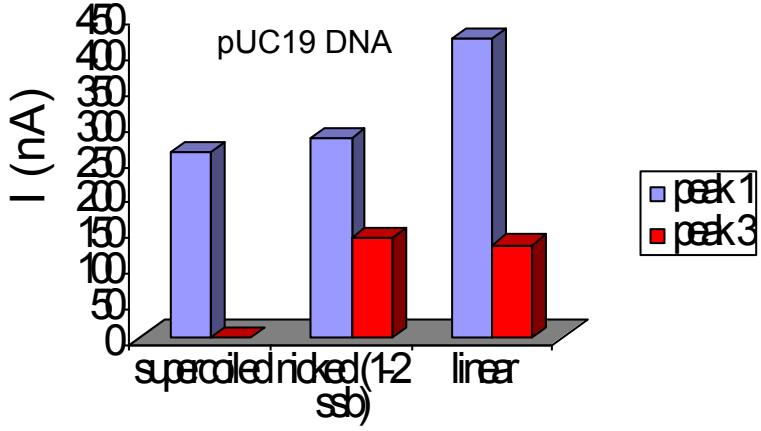
pUC19 DNA
I (nA)
450
400
350
300
250
200
150
100
50
0
supercoiled
nicked (1-2 ssb)
linear
peak 1
peak 3

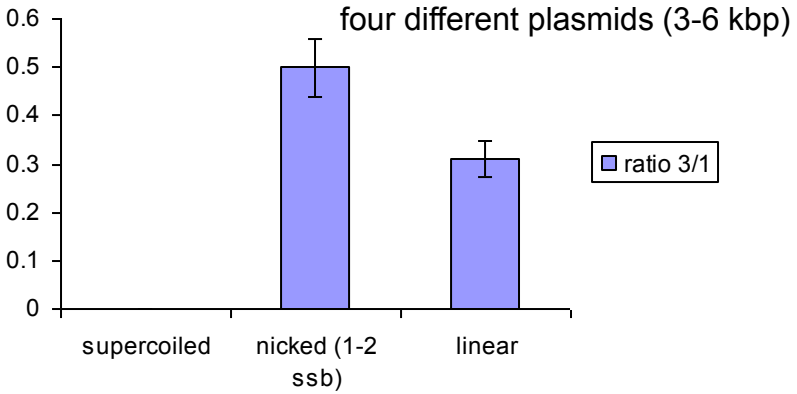
four different plasmids (3-6 kbp)
0.6
0.5
0.4
0.3
0.2
0.1
0
supercoiled
nicked (1-2 ssb)
linear
ratio 3/1

Cleavage of Supercoiled DNA by Deoxyribonuclease I in Solution and at the Electrode Surface

Miroslav Fojta, Tatiana Kubičárová,* and *Emil Paleček*

Institute of Biophysics of the Academy of Sciences of the Czech Republic, Královopolská 135, CZ-612 65 Brno, Czech Republic

monitoring of DNA cleavage in solution using electrochemistry

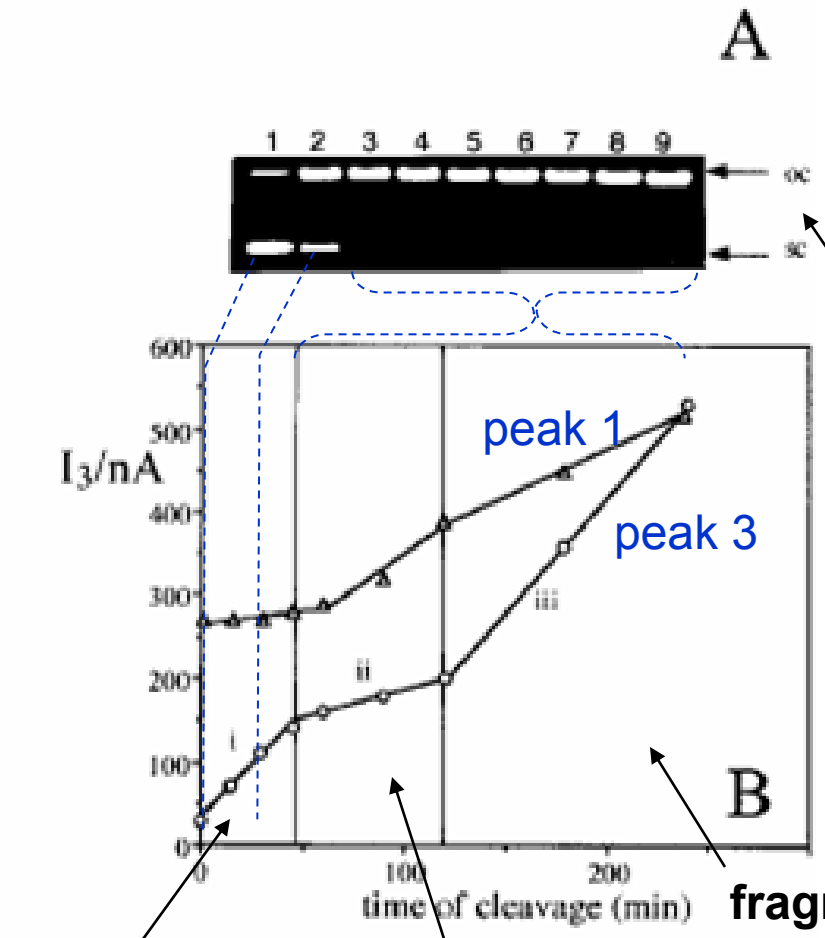

- **DNase I introduces single strand breaks**
- **DNA treated with the enzyme, then adsorbed at HMDE**

agarose gel elfo shows ocDNA as the only product of DNA cleavage during the experiment

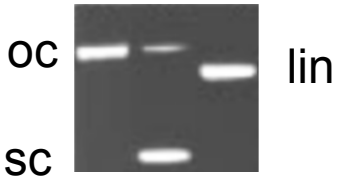

fragmentation upon adsorption

linearization upon adsorption

nicked circular (sb accumulation)

Cleavage of Supercoiled DNA by Deoxyribonuclease I in Solution and at the Electrode Surface

Miroslav Fojta, Tatiana Kubičárová,* and *Emil Paleček*

Institute of Biophysics of the Academy of Sciences of the Czech Republic, Královopolská 135, CZ-612 65 Brno, Czech Republic

different cleavage mechanisms in solution and at the surface?

„solution“: as previous slide

„surface“: DNA adsorbed at HMDE, then treated with the enzyme

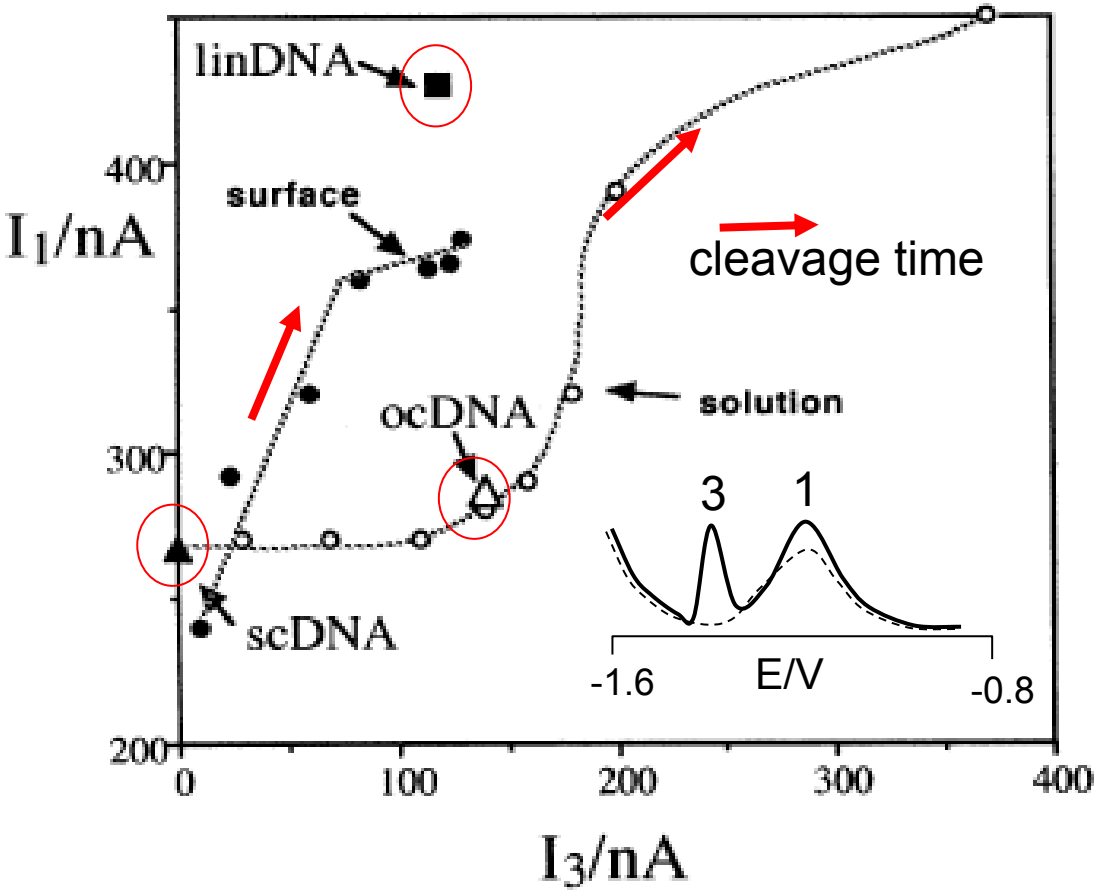

correlation between peak 3 and peak 1 peak heights

Short Communication

Mercury Film Electrode as a Sensor for the Detection of DNA Damage

Tatiana Kubičárová,[+] Miroslav Fojta,[+] Jasmina Vidic,[++] Luděk Havran,[+] and Emil Paleček[+]*

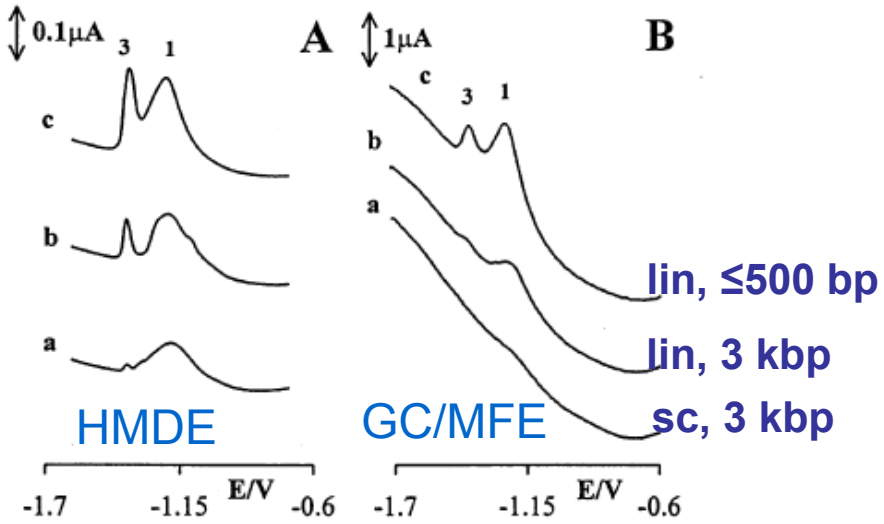

- at the GC/MFE: more pronounced effects of the DNA molecule length
- poor responses of long dsDNAs
- steeper dependence of peak heights on DNA cleavage extent (from the second phase)

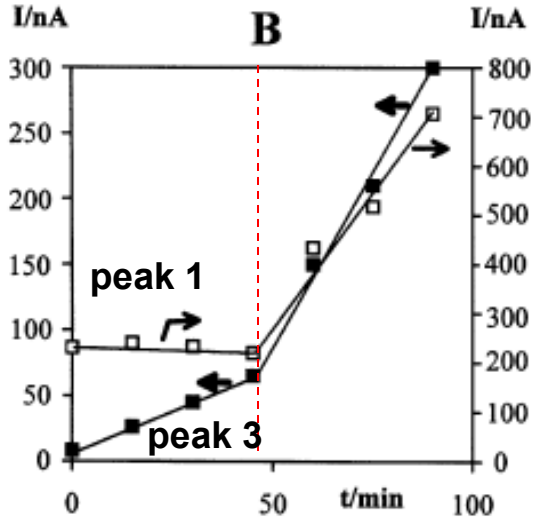

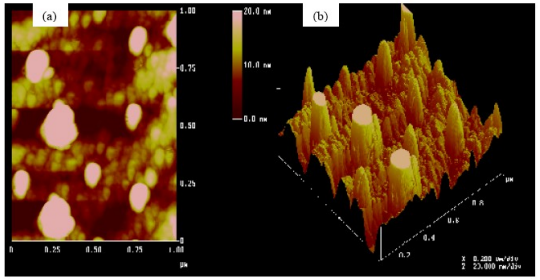

GC/MFE: not a smooth surface like HMDE

long rigid ds DNA: poor contact with the electrode surface

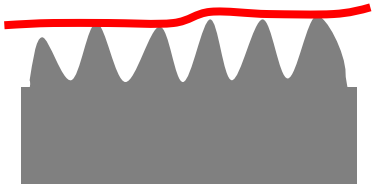

shorter DNA fragments can fit better the surface shape

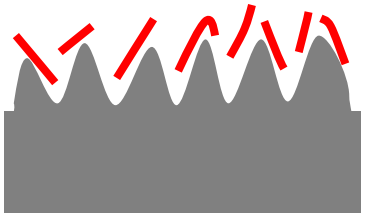

DNA structural changes due to intercalation

Adsorptive Transfer Stripping AC Voltammetry of DNA Complexes with Intercalators

Miroslav Fojta, Luděk Havran, Jana Fulnečková,* and *Tatiana Kubičárová*

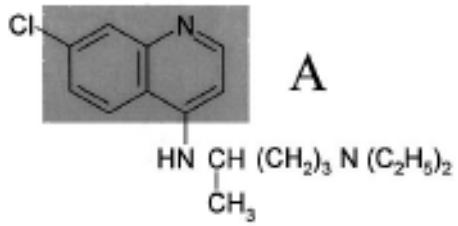

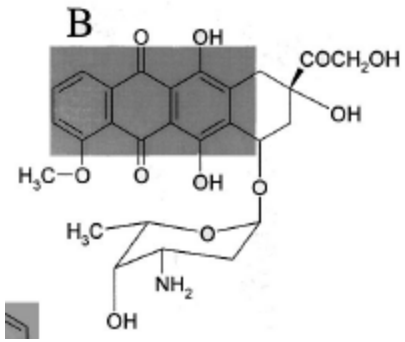

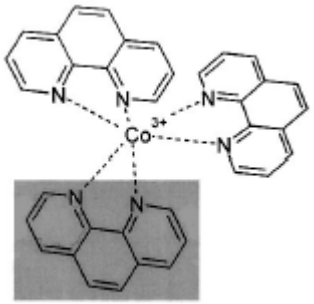

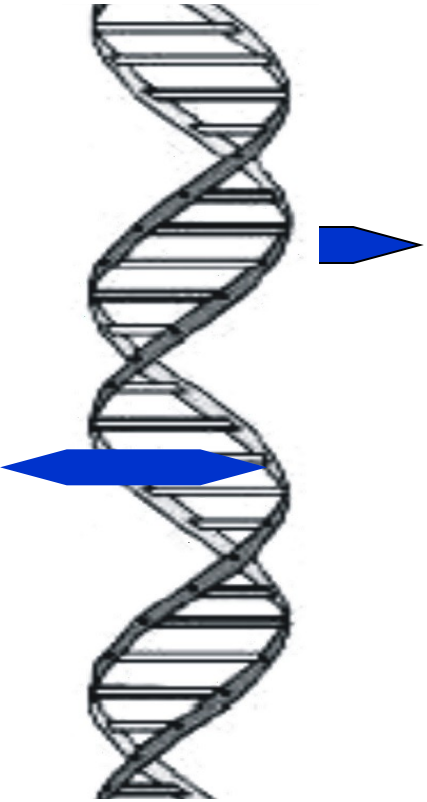

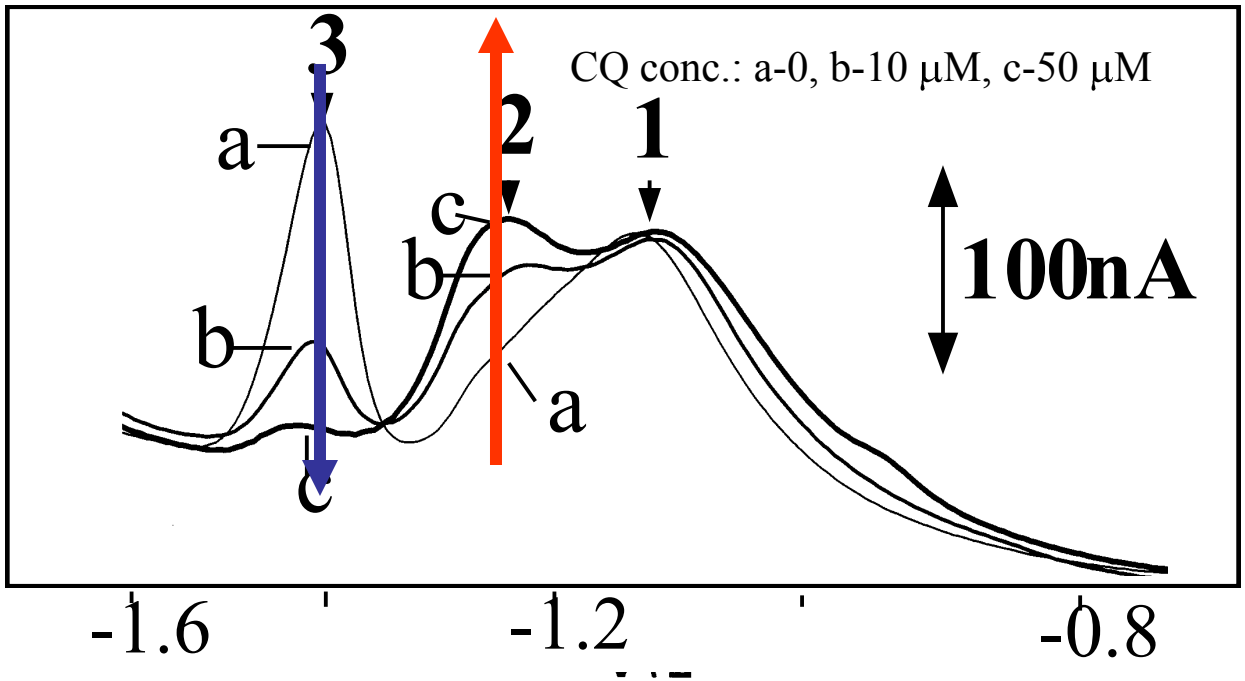

Adsorptive Transfer Stripping AC Voltammetry of DNA Complexes with Intercalators

Miroslav Fojta, Luděk Havran, Jana Fulnečková,* and *Tatiana Kubičárová*

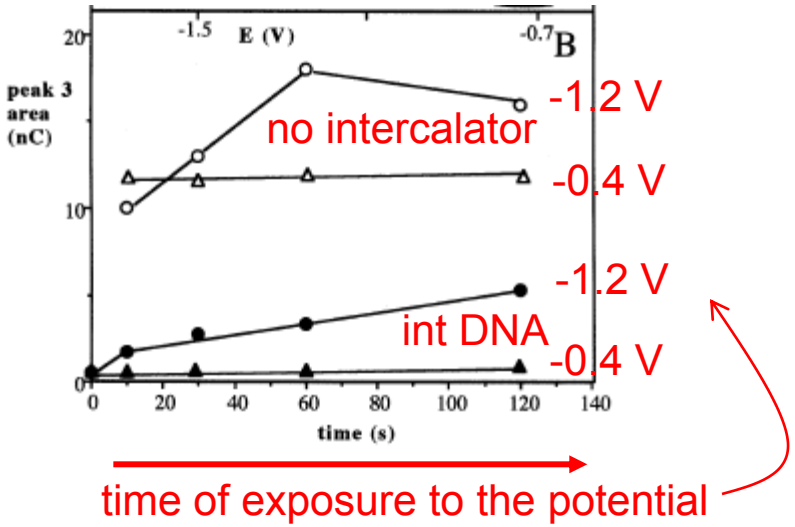

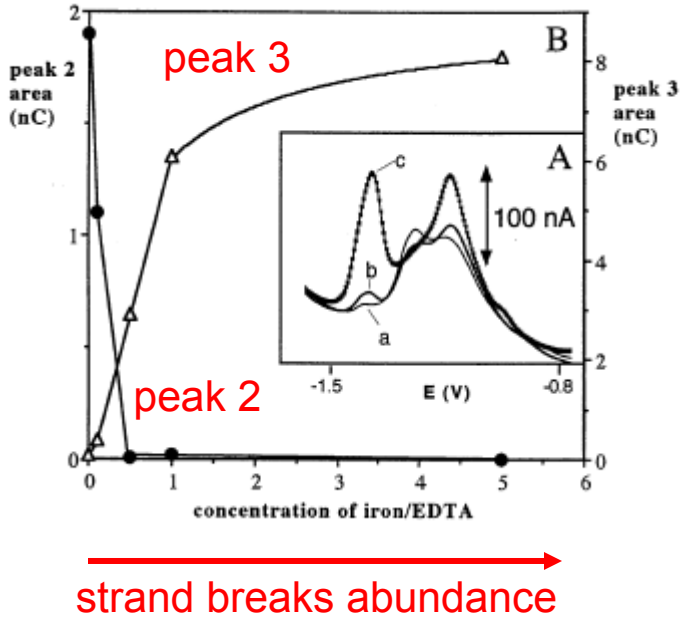

intDNA is more resistant to surface denaturation within the region U

DNA containing numerous strand breaks, adsorbed in the presence of an intercalator, does not yield responses characteristi for intDNA

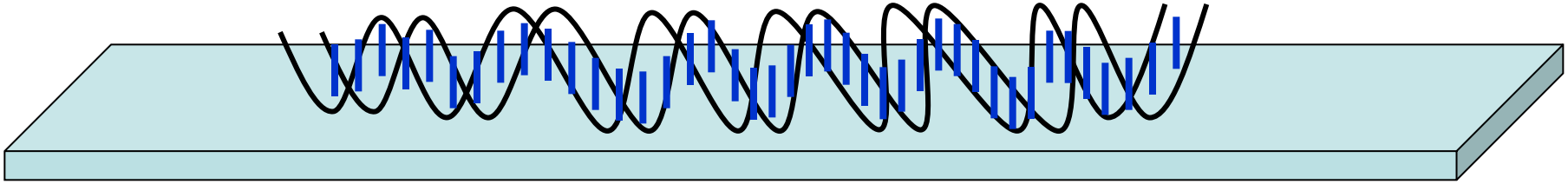

DNA in the absence of intercalator: B-form, bases hidden in the double-helix interior, relatively far from the electrode surface

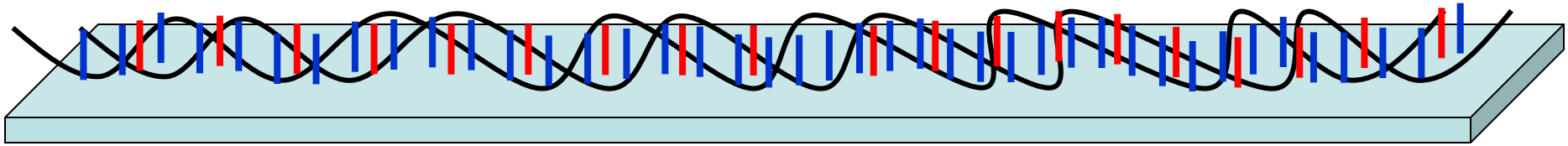

DNA saturated with the intecalator (**intDNA**): untwisted and lengthened double helix, less deep grooves – bases closer to the surface, contacts between the surface and the base pair edges

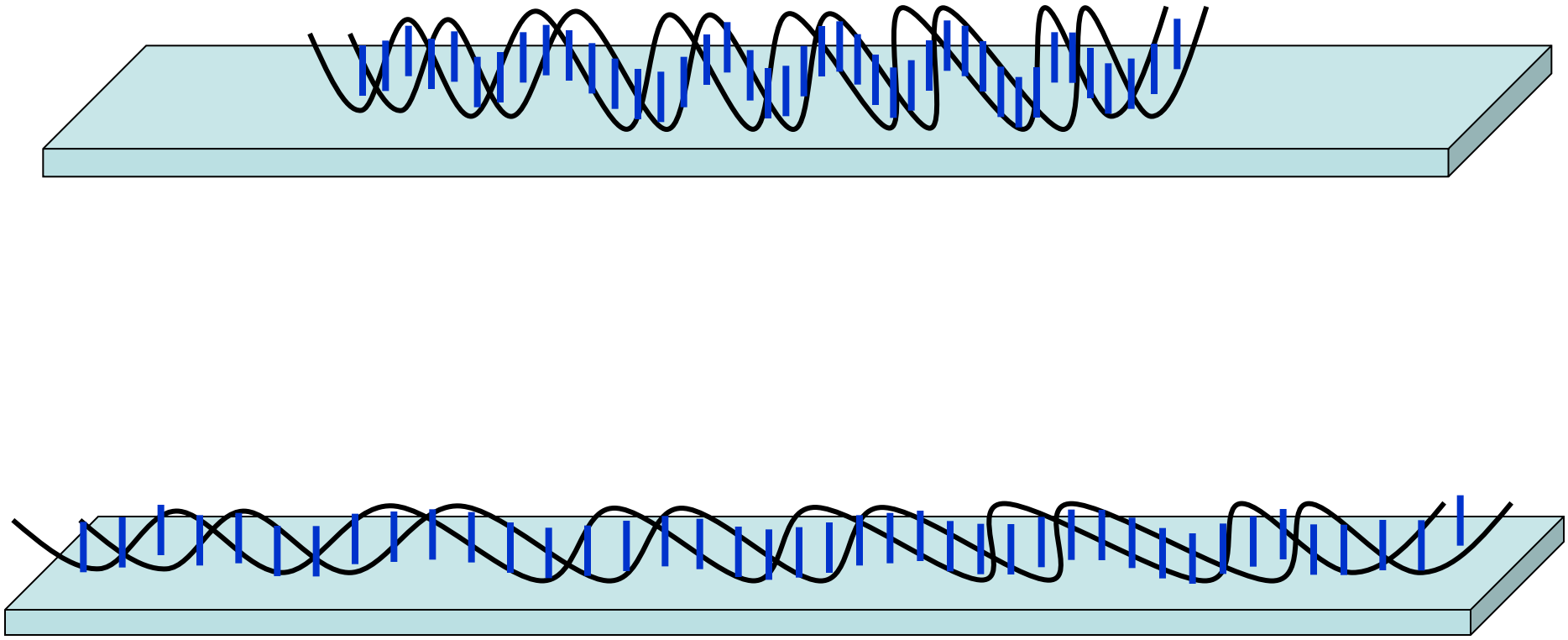

after removal of the intercalator, the intDNA conformation is preserved

the adsorbed untwisted regions of intDNA yield the AV voltammetric peak 2

intDNA with intercalator

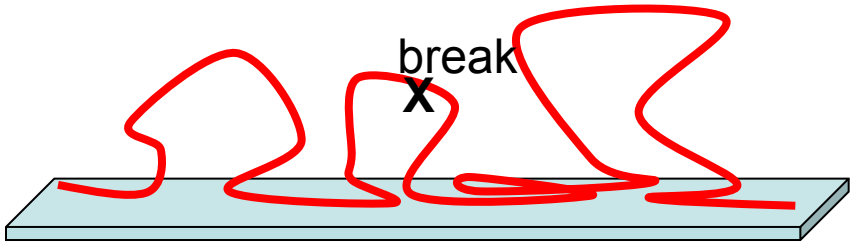

dsDNA without intercalator

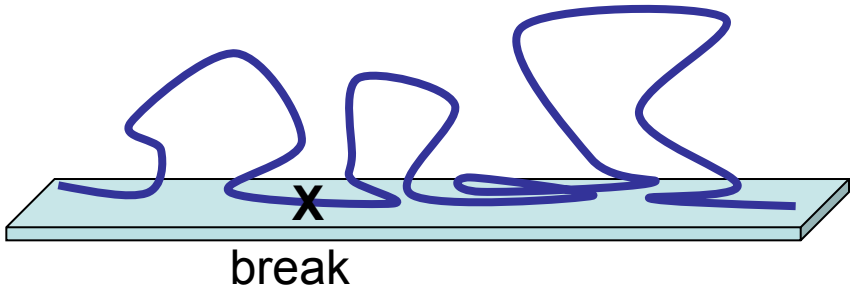

intDNA after intecalator removal

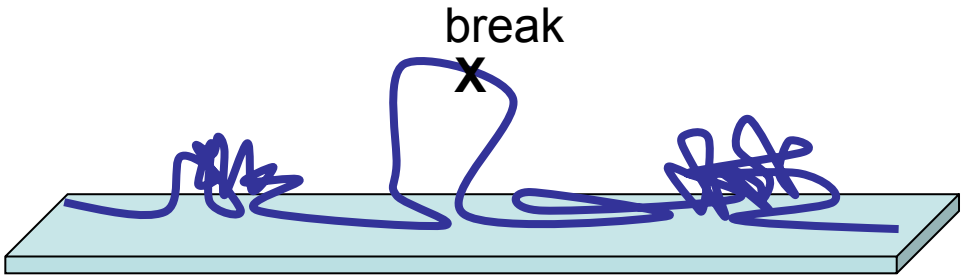

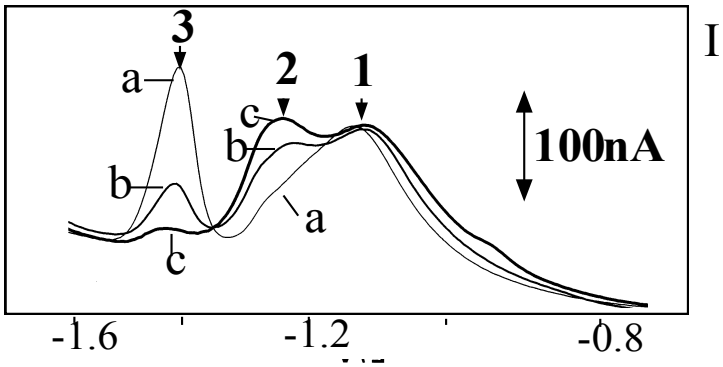

I

dsDNA without intercalator

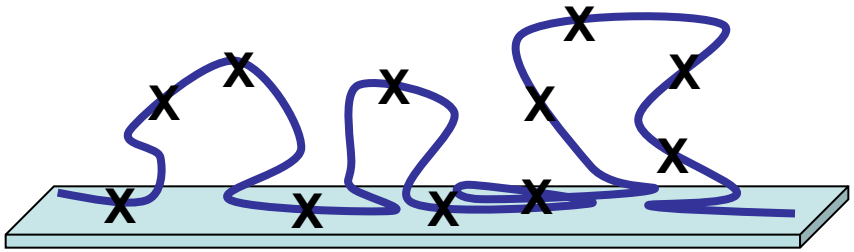

with intercalator

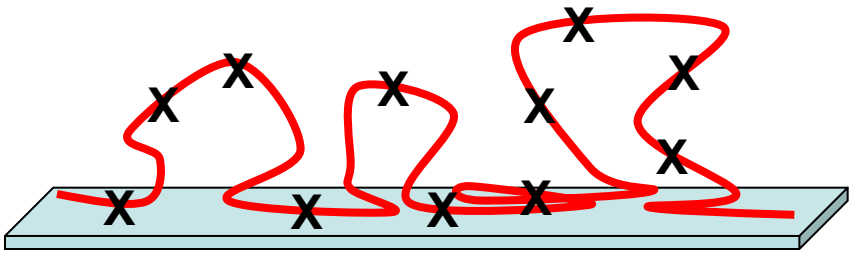

intDNA after intecalator removal

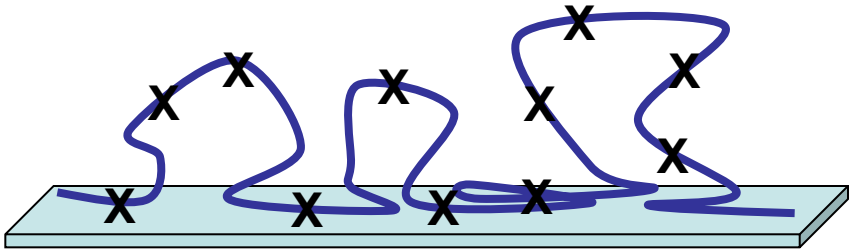

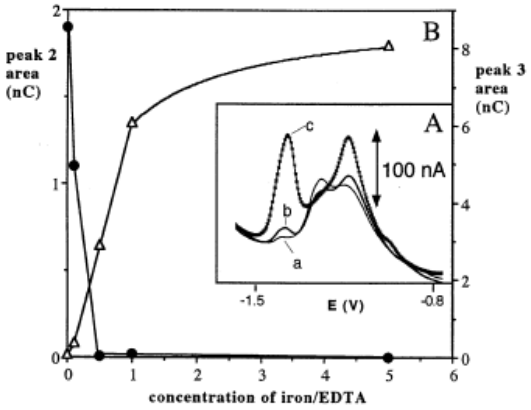

single-stranded oligonucleotides:

effects of nucleobase composition and/or nucleotide sequence

Resolution of Overlapped Reduction Signals in Short Hetero-oligonucleotides by Elimination Voltammetry

Radka Mikelova,[a] Libuse Trnkova,[a] Frantisek Jelen,[b] Vojtech Adam,[c] Rene Kizek [c]*

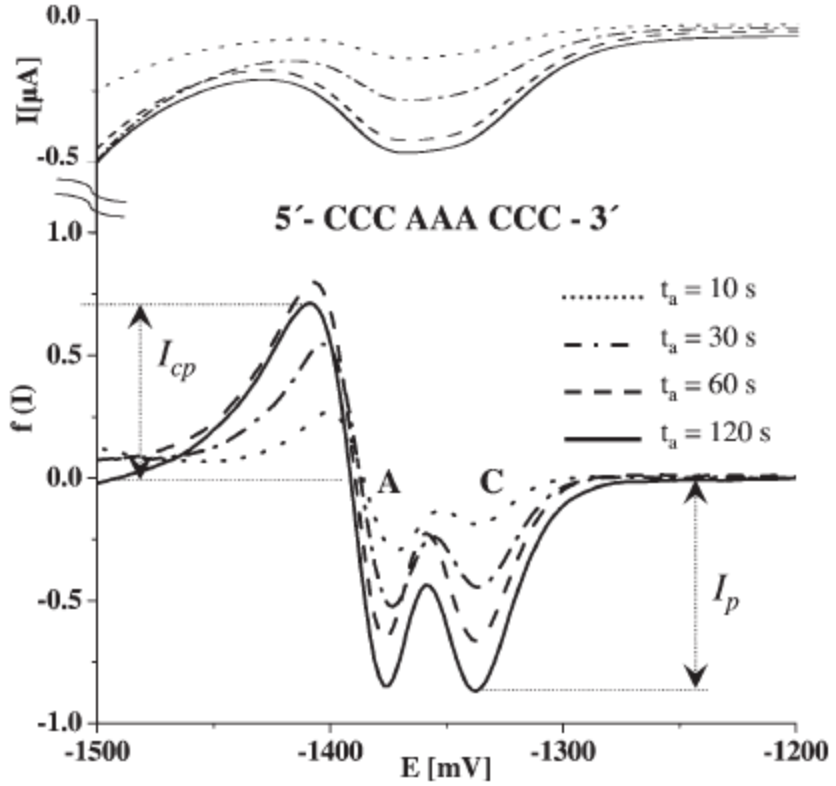

- Dračka, Trnková
- current measured in voltammetry is a sum (linear combination) of partial current components (diffusion, capacitive, kinetic…)
- these componets depend diversely on scan rate
- possibility of numerical elimination of any component based on measurements at several different scan rates
- studies of electrode processes
- separation of overlapped signals

Resolution of Overlapped Reduction Signals in Short Hetero-oligonucleotides by Elimination Voltammetry

Radka Mikelova,[a] Libuse Trnkova,[a] Frantisek Jelen,[b] Vojtech Adam,[c] Rene Kizek [c]*

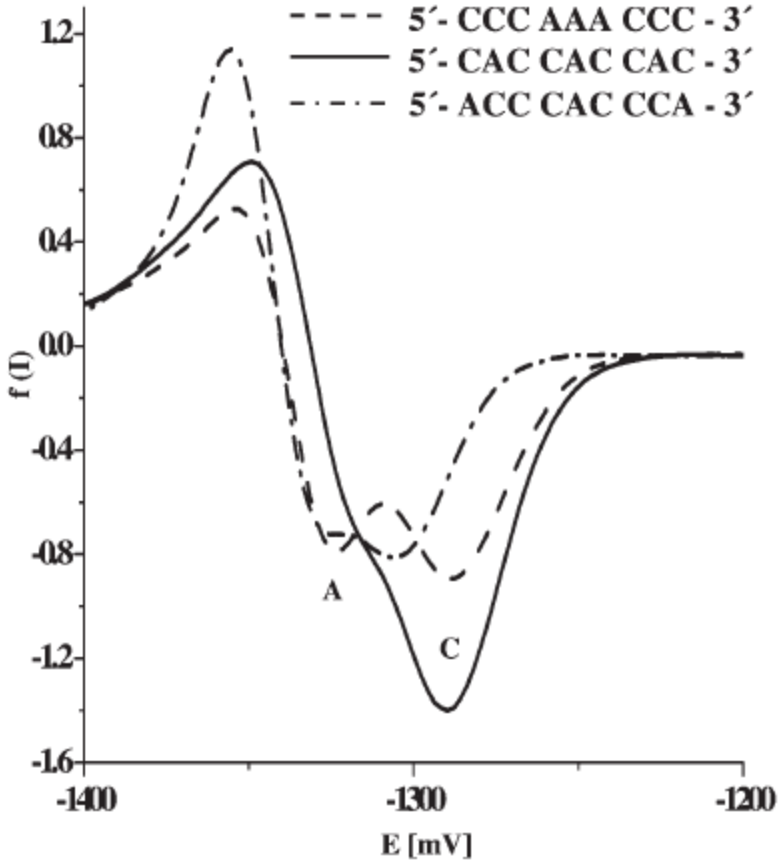

- different EVLS responses for ODNs with identical base content but differing in their sequence

2D condensation of homopyrimidine oligos at mercury-based electrodes

Two-Dimensional Condensation of Pyrimidine Oligonucleotides during Their Self-Assemblies at Mercury Based Surfaces

Stanislav Hasoň, Vladimír Vetterl[1], Miroslav Fojta**

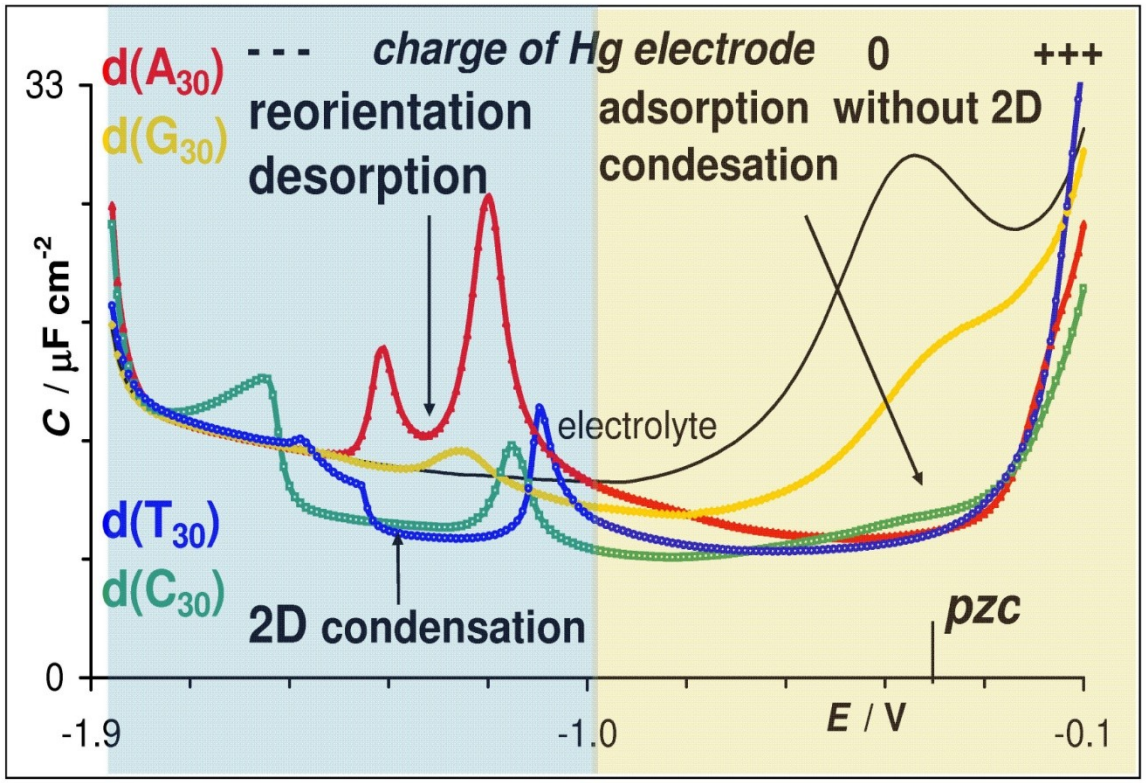

- capacitance pits indicate formation of condesed films
- NA bases, nucleosides, nucleotides for decades known to form such 2D-condensed layers (V. Vetterl)
- up to recently, no observations with DNA, polynucleotides or ODNs
- S. Hason: homopyrimidine ODNs (30 to 90-mers studied) can form such condensed films at negatively charged mercury or amalgam surfaces

transfer (ex-situ) experiment:
the condensed film is formed of reoriented ODN molecules already adsorbed (not due thickening the adsorbed layer by extra molecules form the bulk)

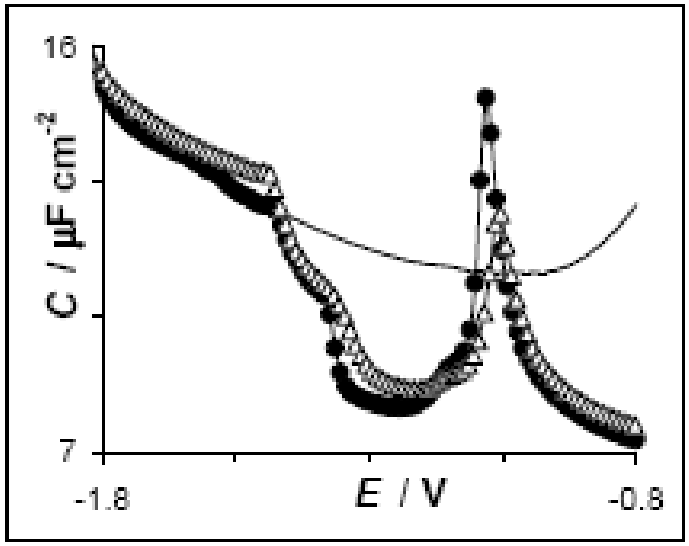

mixed A+G or C+T ODNs

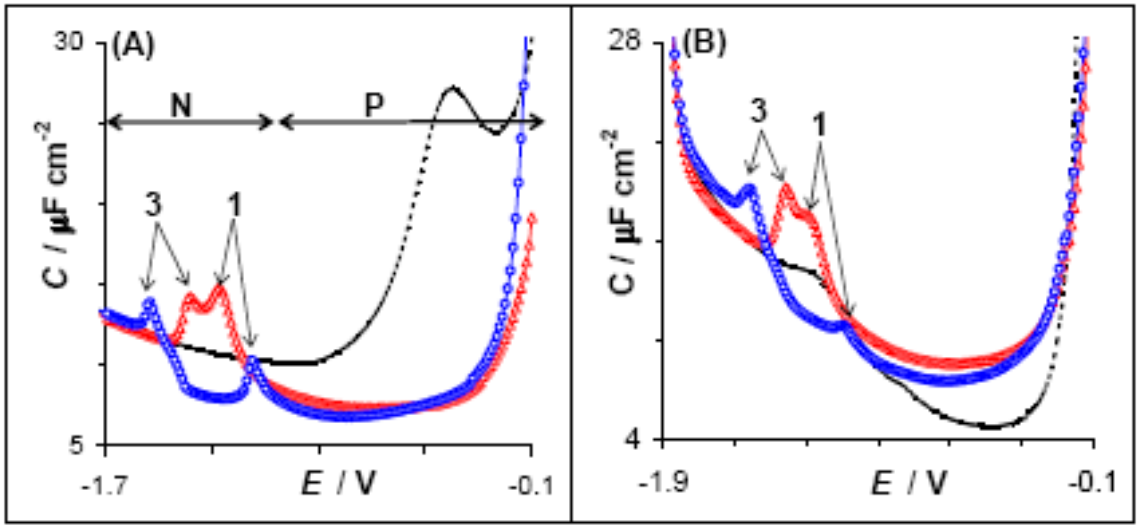

HMDE **silver amalgam electrode**

around pzc: random orientation of the ODN chain

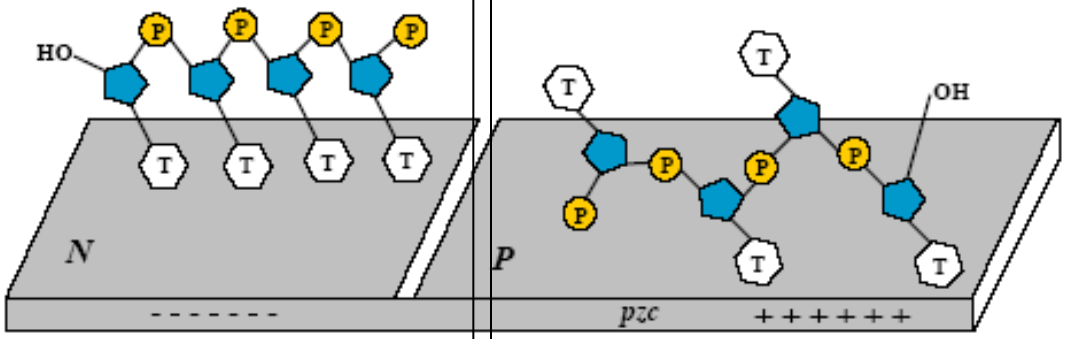

negatively charged surface:
sugar-phosphate backbone repelled
pyrimidine bases udergo self-assembly

these phenomena may affect behavior of ODNs anchored via terminal thiol group